

# **ANALOGUE SELF-INTERFERENCE CANCELLATION IN FULL-DUPLEX RADIOS**

by

Chisala Kabanda

A dissertation submitted to the University of Zambia in partial fulfilment of the requirements for the degree of Master of Engineering in Telecommunications Systems

The University of Zambia

LUSAKA

2019

## DECLARATION

I hereby declare that the work presented in this dissertation is my own, and I have clearly stated where I have consulted the work of others. I further declare that I have not submitted this dissertation at this or any other institution to obtain a degree.

Name: Chisala Kabanda

Signature: .....

Date: .....

## APPROVAL

This dissertation of Chisala Kabanda has been approved as partial fulfilment of the requirements for the award of Master of Engineering in Telecommunications Systems by the University of Zambia.

Examiner 1:..... Signature:..... Date: .....

Examiner 2:..... Signature:..... Date: .....

Examiner 3:..... Signature:..... Date: .....

Chairperson,

Board of

Examiners:..... Signature:..... Date: .....

Supervisor:..... Signature:..... Date: .....

## ABSTRACT

Active analogue self-interference cancellation (AASIC) techniques are used to prevent the saturation of the receiver chain in full-duplex (FD) radios. This is done by cancelling the self-interference (SI) signal before it enters the receiver chain. AASIC techniques are usually implemented together with passive and active digital self-interference cancellation (SIC) techniques.

In this study, an analogue radio frequency (RF) SI canceller that cancels the SI signal before it enters the receiver chain is proposed. The canceller uses an analogue RF circuit with tuneable attenuation, delay, and phase. The analogue RF circuit is implemented together with an RF circulator. The circulator isolates the transmitter chain from the receiver chain. The proposed design aims to reduce the form factor and complexity of the canceller.

The canceller is modelled and simulated in MATLAB/Simulink. The results show that the canceller cancels the SI signal. It achieves 52 dB of SIC using a 20 dBm SI test signal over a bandwidth of 20 MHz. The results also show that the canceller does not affect the signal of interest (SOI).

Keywords: Full-duplex, self-interference, analogue self-interference cancellation.

## **DEDICATION**

*To My Family*

## **ACKNOWLEDGEMENTS**

I would like to thank my supervisor, Dr. C.S. Luboby, for his patience and guidance, and for reading through several drafts of my dissertation. I would also like to thank my co-supervisor, Dr. E. Musonda, for his advice and insight. Finally, I would like to thank my family for their support throughout my studies.

## TABLE OF CONTENTS

<b>DECLARATION</b> .....	<b>ii</b>
<b>APPROVAL</b> .....	<b>iii</b>
<b>ABSTRACT</b> .....	<b>iv</b>
<b>DEDICATION</b> .....	<b>v</b>
<b>ACKNOWLEDGEMENTS</b> .....	<b>vi</b>
<b>LIST OF FIGURES</b> .....	<b>ix</b>
<b>LIST OF TABLES</b> .....	<b>xi</b>
<b>ABBREVIATIONS AND ACRONYMS</b> .....	<b>xii</b>
<b>CHAPTER 1 : INTRODUCTION</b> .....	<b>1</b>
1.1 Background .....	1
1.2 Related Work.....	2
1.3 Problem Statement .....	8
1.4 Aim of Study .....	8
1.5 Objectives .....	9
1.6 Research Questions .....	9
1.7 Significance of Study .....	9
1.8 Scope of Study.....	9
1.9 Organisation of the Dissertation.....	9
<b>CHAPTER 2 : LITERATURE REVIEW</b> .....	<b>11</b>
2.1 Self-Interference Characteristics .....	11
2.1.1 Self-Interference in Separate Antenna Full-Duplex Radios .....	11
2.1.2 Self-Interference in Single Antenna Full-Duplex Radios.....	12

2.2 Self-Interference Cancellation.....	13
2.2.1 Passive Self-Interference Cancellation .....	14
2.2.2 Active Analogue Self-Interference Cancellation.....	19
2.2.3 Active Digital Self-Interference Cancellation .....	22
2.2.4 Self-Interference Cancellation Summary.....	25
2.3 Direct Conversion Receiver .....	26
<b>CHAPTER 3 : METHODOLOGY.....</b>	<b>30</b>
3.1 Signal Model .....	30
3.2 Proposed Analogue RF Self-Interference Canceller .....	31
3.3 System Simulation.....	34
<b>CHAPTER 4 : RESULTS AND DISCUSSION .....</b>	<b>40</b>
4.1 Self-Interference Cancellation Performance .....	40
4.1.1 Self-Interference Cancellation in the Absence of the Signal of Interest....	40
4.1.2 Self-Interference Cancellation in the Presence of the Signal of Interest ...	43
4.2 Self-Interference Cancellation Performance Comparison.....	46
<b>CHAPTER 5 : CONCLUSION AND RECOMMENDATIONS .....</b>	<b>49</b>
5.1 Conclusion.....	49
5.2 Recommendations and Future Work .....	50
<b>REFERENCES.....</b>	<b>51</b>
<b>APPENDIX: SYSTEM SIMULATION CONFIGURATIONS.....</b>	<b>56</b>

## LIST OF FIGURES

Figure 1.1: Comparison of TDD and FDD with FD Communication .....	1
Figure 1.2: AASIC Using QHx220 Noise Cancelling Chip .....	5
Figure 1.3: AASIC Using a Tuneable Analogue RF Circuit and a Balun .....	5
Figure 1.4: AASIC Using an Auxiliary TX Chain.....	6
Figure 1.5: AASIC Using Multi-tap Tuneable Analogue RF Circuit .....	7
Figure 2.1: Separate Antenna FD Radio .....	12
Figure 2.2: Single Antenna FD Radio with a Circulator.....	12
Figure 2.3: PSIC Using Antenna Separation Technique.....	15
Figure 2.4: PSIC Using Antenna Placement Technique .....	15
Figure 2.5: Directional Antennas .....	16
Figure 2.6: Cross Polarisation using Dual Polarised Antennas .....	17
Figure 2.7: PSIC Using a Dual Polarised Antenna .....	17
Figure 2.8: PSIC Using a Circulator .....	18
Figure 2.9: EBD Operation: a)Transmission b)Reception.....	19
Figure 2.10: AASIC Using an Auxiliary TX Chain.....	20
Figure 2.11: AASIC Using a Tuneable RF Circuit .....	21
Figure 2.12: ADSIC Using a Digital Baseband Circuit .....	23
Figure 2.13: ADSIC Using an Auxiliary RX Chain .....	25
Figure 2.14: Summary of SIC Techniques.....	26
Figure 2.15: Direct Conversion Receiver.....	27
Figure 3.1: Proposed Analogue RF Self-Interference Canceller .....	31
Figure 3.2: Model Used in System Simulation .....	35
Figure 3.3: SI Source Model .....	36
Figure 3.4: SOI Source Model .....	36

Figure 3.5: Circulator Model.....	37
Figure 3.6: Attenuator and Delay Model .....	38
Figure 3.7: Rayleigh Fading Channel Model.....	38
Figure 3.8: Analogue RF SI Canceller Model .....	38
Figure 3.9: Analogue RF SI Canceller Signal Path Model .....	39
Figure 4.1: Input SI Signal .....	41
Figure 4.2: PSIC Performance in the Absence of the SOI.....	41
Figure 4.3: AASIC Performance in the Absence of the SOI .....	42
Figure 4.4: Input SI signal and SOI .....	43
Figure 4.5: PSIC Performance in the Presence of the SOI .....	44
Figure 4.6: AASIC Performance in the Presence of the SOI.....	44
Figure 4.7: Superimposition of SOI on Received Signal After AASIC .....	45

## LIST OF TABLES

Table 4.1: SIC Performance Summary in the Absence of the SOI.....	42
Table 4.2: SIC Performance Summary in the Presence of the SOI. ....	46
Table 4.3: Performance Comparison Summary. ....	48

## ABBREVIATIONS AND ACRONYMS

5G	Fifth Generation
AASIC	Active Analogue Self-Interference Cancellation
ADC	Analogue to Digital Converter
ADSIC	Active Digital Self-Interference Cancellation
AMP	Amplifier
Balun	Balanced/Unbalanced Transformer
BPSK	Binary Phase Shift Keying
CPLX	Complex
CSI	Channel State Information
DAC	Digital Analogue Converter
dB	Decibel
dBm	Decibel-Milliwatts
DCR	Direct Conversion Receiver
DSP	Digital Signal Processing
FD	Full-Duplex
FDD	Frequency Division Duplex
FFT	Fast Fourier Transform
FIR	Finite Impulse Response
I	In-Phase
IF	Intermediate Frequency
IQ	In-Phase/Quadrature
LMS	Least Mean Squares
LNA	Low Noise Amplifier
LO	Local Oscillator

LOS	Line of Sight
LPF	Low-pass Filter
MAC	Media Access Control
MIMO	Multiple-Inputs Multiple-Outputs
NLOS	Non-Line of Sight
OQPSK	Offset Quadrature Phase-Shift Keying
PA	Power Amplifier
PSIC	Passive Self-Interference Cancellation
Q	Quadrature
RF	Radio Frequency
RX	Receiver
SI	Self-Interference
SIC	Self-Interference Cancellation
SOI	Signal of Interest
TDD	Time Division Duplex
TX	Transmitter
VFD	Variable Fractional Delay
VGA	Variable Gain Amplifier
VM	Vector Modulator

## CHAPTER 1 : INTRODUCTION

### 1.1 Background

Full-Duplex (FD) communication is a technology that has been proposed to improve spectral efficiency in wireless communication systems [1]. In FD communication, the radio simultaneously transmits and receives at the same frequency [2]. In contrast, conventional wireless communication systems do not simultaneously transmit and receive at the same frequency because of the self-interference (SI) that results [3]. Instead, they separate transmission and reception using time division duplex (TDD) or frequency division duplex (FDD) [2], [4]. In TDD, different timeslots are used to transmit and receive at the same frequency, whereas in FDD, different frequencies are used to transmit and receive at the same time [3]. Figure 1.1 shows a comparison of TDD and FDD with FD communication.

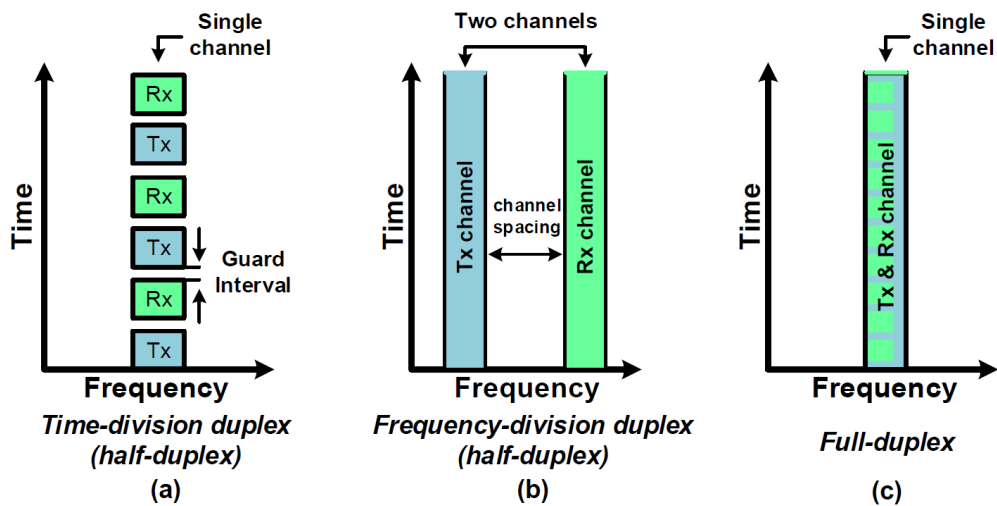


Figure 1.1: Comparison of TDD and FDD with FD Communication [4].

Compared with FDD and TDD, FD communication has the potential to double the spectral efficiency of wireless communication systems [1]. FD communication could also provide solutions to other problems faced in wireless communication systems.

These problems include the hidden node problem [5], [6], delays in multi-hop stations [7], and spectrum sensing in cognitive radios [8].

The main challenge in implementing FD communication is the SI that results when a radio simultaneously transmits and receives at the same frequency [1]–[10]. The presence of the SI signal in the received signal adversely affects the performance of the receiver (RX) chain because the SI signal is usually 60–100 dB stronger than the signal of interest (SOI) [9].

## **1.2 Related Work**

A considerable amount of research has been on FD communication in the last few years. Most of this research consists of surveys on FD communication [1], [11]–[15], and the implementation of SIC techniques [1]–[10].

Surveys on existing FD communication mainly look at the basic principles of FD communication, existing SIC techniques, and applications of FD communication. To illustrate, the authors of [1] reviewed the main concepts of FD communication. They outlined the motivation for FD communication and some of its applications. Furthermore, they identified SI as the main challenge in implementing FD communication and categorised existing SIC techniques into three main groups. These categories are propagation-domain, analogue-circuit domain, and digital-domain SIC techniques. They noted that proposed FD radios use a combination SIC techniques. The authors then considered three basic wireless communication topologies that could benefit from FD communication. These are relay, bidirectional, and base station topologies. They also outlined research challenges and opportunities in FD communication.

In [11], the authors looked at FD relaying as a potential application of FD communication. The authors noted that significant challenges must be addressed before deploying FD communication. These challenges include small form factor FD device design, channel modelling and estimation, cross-layer/joint resource management, interference management, and security. The authors then discussed SIC in FD relaying. They noted that a combination of propagation, analogue-circuit, and digital domain SIC techniques is required to implement SIC in FD relay systems. The authors also discussed information-theoretic performance analysis, fundamental design issues, challenges, and research opportunities in FD relaying.

In [12], the authors introduced the basic concepts of FD communication systems. They also reviewed SIC techniques and discussed the effects of FD communication on the system performance of three network topologies. These are bidirectional, relay, and cellular network topologies. The authors then compared the performance of FD communication systems with that of conventional half-duplex (HD) systems, examined the development of media access control (MAC) protocols for FD communication in infrastructure-based and ad hoc networks, and discussed research challenges and opportunities in FD communication. They concluded the survey by outlining the advantages of FD communication in different applications.

The authors of [13] gave a brief survey on FD relaying. They first discussed the importance of FD communication and the associated SI. They then examined SIC techniques and assessed developments in FD relaying. They concluded the survey with a discussion on the importance of FD relaying in 5G networks. In [14], the authors presented a comprehensive list of SIC techniques and outlined their advantages and disadvantages. They classified the SIC techniques into three categories: passive

suppression, analogue cancellation and digital cancellation. They also analysed the main impairments that affect SIC. Finally, they outlined a variety of new directions and open problems in FD communication.

In [15], the authors also presented a comprehensive survey of SIC techniques and examined their performance, strengths, and weaknesses. They categorised the proposed SIC techniques and quantified the amount of SIC required for various generations of mobile cellular systems.

The surveys reviewed above have identified SI as the main challenge in implementing FD communication [1], [11]–[15]. They have also noted that a combination of passive, active analogue and active digital SIC techniques is needed to effectively cancel the SI signal [1], [11]–[15]. This study focused on active analogue SIC (AASIC) in FD radios.

Several AASIC techniques have been proposed in literature. The authors of [5] presented an AASIC technique that used a QHx220 noise cancelling chip, two transmit antennas and one receive antenna, as shown in Figure 1.2. The design separated the two transmit antennas by a distance of  $d$  and  $d+\lambda/2$  away from the receive antenna. The QHx220 chip took the known SI and received signals as inputs and outputted the received signal with the SI subtracted. The chip changed the amplitude and phase of the reference signal to match the SI signal in the received signal. The system provided 20 dB of AASIC. However, the combination of passive and active analogue SIC techniques used in [5] is only suitable for narrowband signals as the performance of the system degrades with increasing bandwidth.

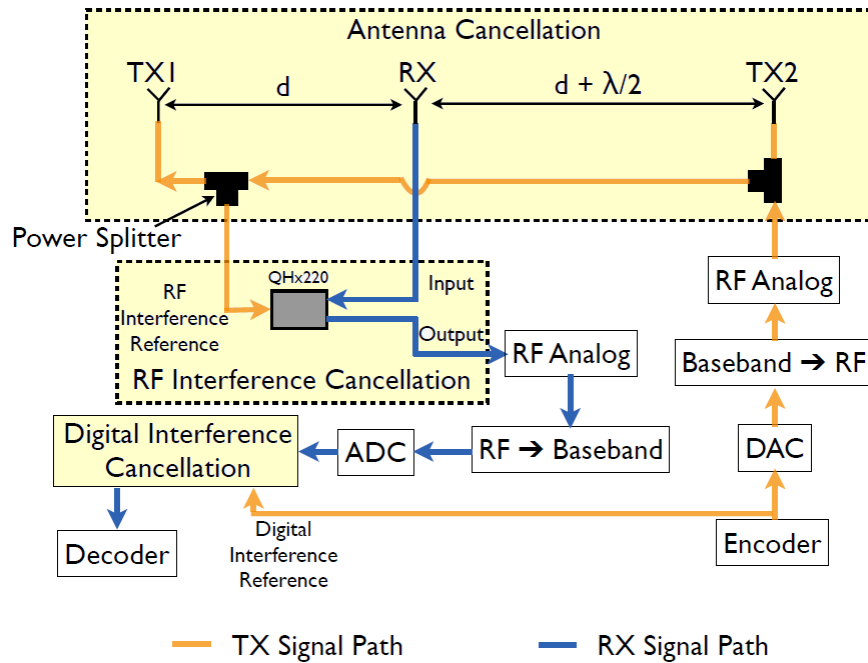


Figure 1.2: AASIC Using a QHx220 Noise Cancelling Chip [5].

In [16], the authors used a tunable RF circuit with a Balanced/unbalanced (Balun) transformer to implement AASIC, as shown in Figure 1.3. They used separate antennas to transmit and receive and tapped the reference signal from the output of the transmitter (TX) chain.

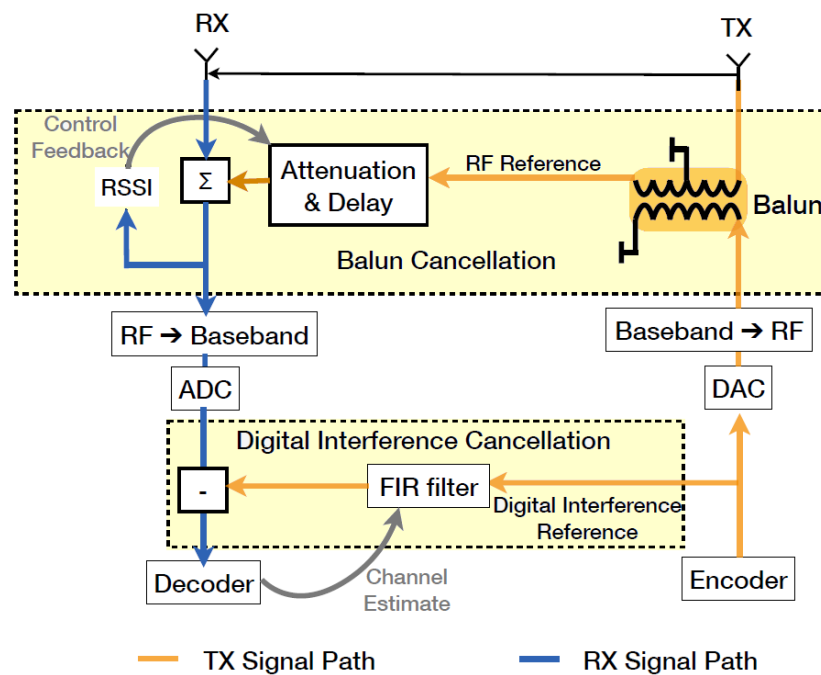


Figure 1.3: AASIC Using a Tuneable Analogue RF Circuit and a Balun [16].

They then used a Balun to get the inverse of the SI signal from the reference signal and fed it into an analogue RF circuit to get the cancellation signal. The RF circuit consisted of one tap with a variable attenuator and delay line. The system provided 45 dB of AASIC. However, the Balun must accurately invert the reference signal for the system to cancel the SI signal effectively.

The authors of [17] used an auxiliary TX chain to implement AASIC, as shown in Figure 1.4. The design used a circulator to isolate the TX chain from the RX chain. The reference signal was tapped from the digital baseband of the TX chain and processed using linear and non-linear pre-distortion signal models. The resulting signal was then up-converted to analogue RF where SIC took place. This design achieved at least 28 dB of AASIC. The main disadvantages of this AASIC technique are that an auxiliary TX chain is required and all impairments in the main TX chain have to be accurately estimated in the signal model.

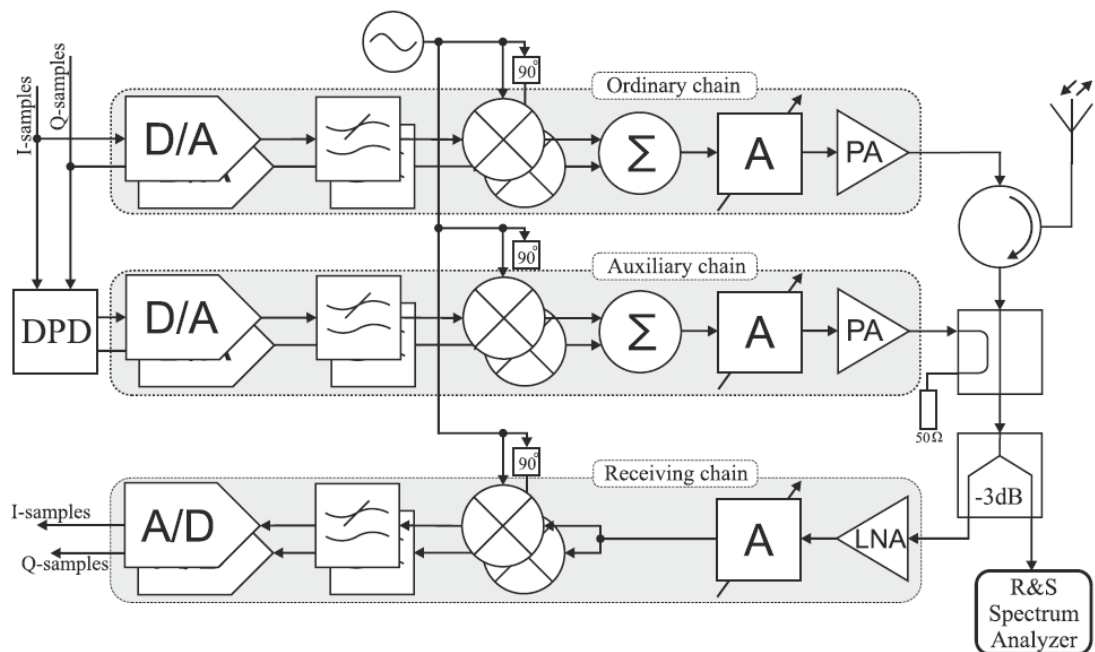


Figure 1.4: AASIC Using an Auxiliary TX Chain [17].

In [18], the authors presented an AASIC technique that used a 16-tap tuneable RF circuit with tuneable attenuators and fixed delays. The design used a circulator to isolate the TX chain from the RX chain, as shown in Figure 1.5. The RF circuit cancelled the two primary SI components in FD radios that use circulators. The two SI components had average delay times of 400 ps and 1.4 ns, respectively. Eight of the 16 lines in [18] had delays centred around 400 ps and cancelled the component that leaked through the circulator. The other eight had delays centred around 1.4 ns and cancelled the SI component that was reflected by the antenna due to impedance mismatch. The design achieved 57 dB of AASIC over a bandwidth of 20 MHz and 47 dB over a bandwidth of 80 MHz channel. The main disadvantage of this AASIC technique is that it uses a large number of taps.

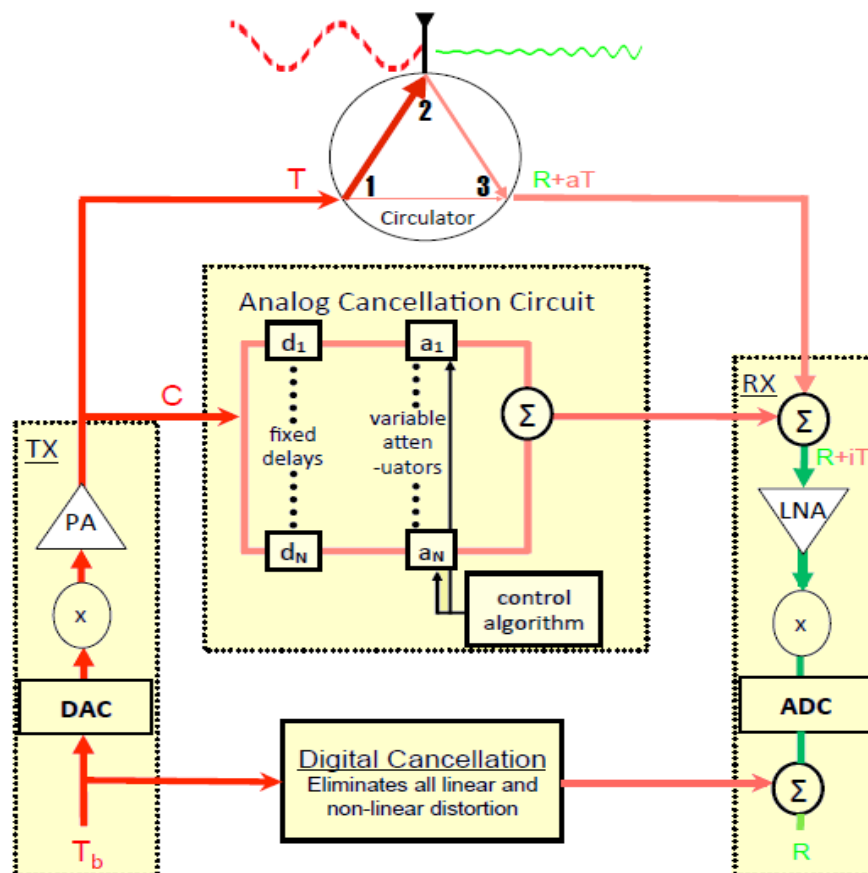


Figure 1.5: AASIC Using a Multi-tap Tuneable Analogue RF Circuit [18].

The authors of [19] proposed a technique that used a vector modulator (VM) and a fixed delay to implement AASIC. They tapped the reference signal from the output of the power amplifier (PA) of the TX chain and fed it into an analogue RF circuit where they delayed it using a fixed delay. They then attenuated and rotated the signal using a VM. Finally, they subtracted the resulting signal from the received signal before it entered the RX chain. This technique achieved an AASIC value of 36 dB. The main disadvantage of this AASIC technique is that the fixed delay has to be carefully set for the system to remove the intended SI components.

### **1.3 Problem Statement**

FD communication has the potential to double the spectral efficiency of wireless communication systems [1]. It also has the potential to solve other problems in wireless communication systems such as the hidden node problem [5], [6], delays in multi-hop stations [7] and spectrum sensing in cognitive radios [8]. However, simultaneously transmitting and receiving at the same frequency results in SI in the RX chain [3]. Therefore, there is a need to design radios that can cancel the SI signal to realise the potential benefits of FD communication [6], [15].

Various SI cancelling radio designs have been proposed in literature. However, most of these designs use complex analogue RF SI cancellers to implement AASIC. These cancellers are not suitable for small form factor devices because of their size and complexity.

### **1.4 Aim of Study**

The aim of this study was to propose a design of an analogue RF canceller that utilises a simple design and can provide sufficient SIC performance before the RX chain.

## **1.5 Objectives**

The objectives of this study were:

1. To propose a design for an analogue RF SI canceller.
2. To analyse the SIC performance of the proposed analogue RF SI canceller.
3. To compare the SIC performance of the proposed analogue RF SI canceller with the SIC performance of other canceller designs.

## **1.6 Research Questions**

The following research questions were answered in this study to achieve the above objectives:

1. What are the characteristics of the proposed analogue RF SI canceller?
2. What is the SIC performance of the proposed analogue RF SI canceller?
3. How does the SIC performance of the proposed analogue RF SI canceller compare with the SIC performance of other canceller designs?

## **1.7 Significance of Study**

FD communication has potential to double the spectral efficiency of wireless communication systems. Therefore, designing simple analogue RF SI cancellers would enable FD communication to be applied to small form factor devices.

## **1.8 Scope of Study**

This study only considers the system-level design of an analogue RF SI canceller that can be used to cancel the SI signal before the RX chain.

## **1.9 Organisation of the Dissertation**

This dissertation is organised as follows: Chapter 2 presents the literature review of this study. It looks at SI in FD radios, the types of SIC techniques, and the direct conversion RX (DCR) architecture. Chapter 3 presents the methodology used in this

study. It outlines the methods and materials used to design and simulate the proposed analogue RF SI canceller. Chapter 4 presents the SIC performance of the proposed analogue RF SI canceller and compares it with the SIC performance of other canceller designs. Finally, Chapter 5 concludes the dissertation, gives the recommendations of the study and discusses future work.

## **CHAPTER 2 : LITERATURE REVIEW**

This chapter reviews the literature relevant to this study. Section 2.1 looks at the characteristics of self-interference (SI) in full-duplex (FD) radios. Section 2.2 looks at self-interference cancellation (SIC) techniques, and section 2.3 looks at the direct conversion receiver (DCR) architecture.

### **2.1 Self-Interference Characteristics**

SI occurs when a radio simultaneously transmits and receives using the same frequency band [10],[20]. The SI signal received by the receiver (RX) is much stronger than the signal of interest (SOI) since it is generated locally [17]. It is usually 60-100 dB stronger than the SOI [9]. Furthermore, the SI signal that is received at input of the RX chain is different from the known transmitted baseband signal that causes it [21]. The SI signal is a combination of the transmitted baseband signal, distorted versions of the transmitted baseband signal and noise [18]. The distortions are caused by the non-linear components in the TX chain and the channel [18], [21].

The SI signal observed at the input of the RX also depends on the antenna configuration used in the FD radio [6]. Two of the most commonly used antenna configurations in FD radios are the separate antenna configuration and single/shared antenna configuration [22]. The following two sections look at the characteristics of SI in FD radios that use these two antenna configurations.

#### **2.1.1 Self-Interference in Separate Antenna Full-Duplex Radios**

In FD radios that use separate antennas to transmit and receive, the SI signal consists of two components, as shown in Figure 2.1. A line of sight (LOS) component and a non-line of sight (NLOS) component [20]. The LOS component consists of the transmitted RF signal that is directly coupled to the local RX, while the NLOS

component consists of multipath reflections of the transmitted RF signal from the environment [20],[23].

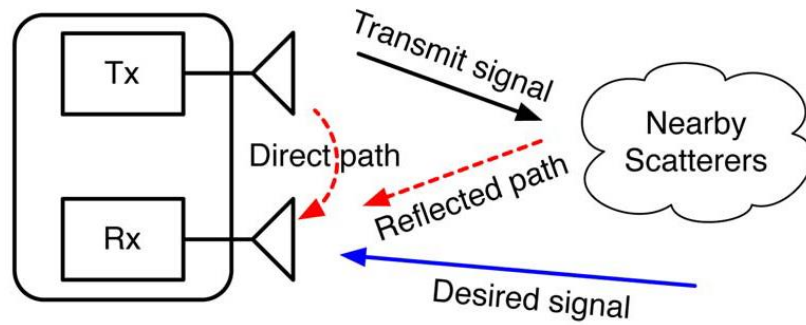


Figure 2.1: Separate Antenna FD Radio [1].

### 2.1.2 Self-Interference in Single Antenna Full-Duplex Radios

Single antenna FD radios use one antenna to transmit and receive. An isolation device is usually used to isolate the TX chain from the RX chain [24], [25], [26], [27]. Figure 2.2 shows a single antenna FD radio that uses a circulator to isolate the TX chain from the RX chain.

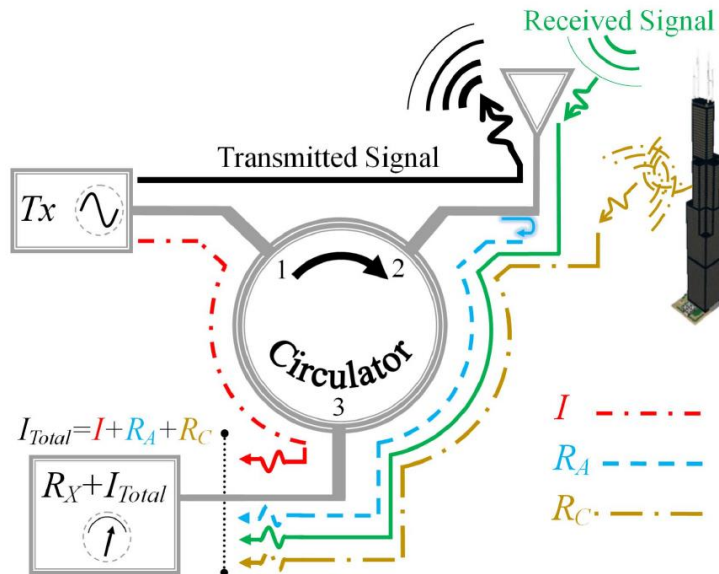


Figure 2.2: Single Antenna FD Radio with a Circulator [25].

The SI signal in a single antenna FD radio consists of three components [25], [28]:

1. The transmitted RF signal that leaks through the isolation device from the TX chain to the RX chain;
2. The transmitted RF signal that the antenna reflects due to impedance mismatch;
3. The NLOS component which consists of multipath reflections of the transmitted RF signal from the environment.

Therefore, the SI signal in the FD radio shown in Figure 2.2 is given by:

$$I_{Total} = I + R_A + R_C \quad (2.1)$$

where  $I$  is the SI component that leaks through the circulator,  $R_A$  is the SI component that the antenna reflects due to impedance mismatch, and  $R_C$  are the multipath reflections from the environment [25]. The leakage through the circulator and the reflection from the antenna have significantly more power and shorter delays than the multipath reflections from the environment [24].

Single antenna FD radios commonly use circulators as isolation devices [22],[25],[26]. A circulator is a passive, multi-port ferromagnetic device in which a radio frequency signal entering one port is transmitted to the next port in a rotational direction [18], [29]. To illustrate, the signal in the circulator in Figure 2.2 rotates in the clockwise direction. However, circulators do not provide perfect isolation among their ports in the reverse direction [18]. As a result, part of the signal propagates in the reverse direction [25]. Circulators provide 20-60 dB isolation in the reverse direction depending on their size and cost [30].

## 2.2 Self-Interference Cancellation

The magnitude of the SI signal is more than that of the SOI [9], [17]. Its presence in the received signal makes the recovery of the SOI very difficult and could damage the

RX chain [31]. SIC techniques are used to cancel the SI signal in FD radios so that the SOI can be recovered [32], [33].

The amount of SIC required depends on the technology in question. For example, the amount of SIC required in a Wi-Fi radio transmitting at 20 dBm and has an RX noise floor of -90 dBm is 110 dB [33]. A variety of SIC techniques have been proposed in literature. SIC techniques are generally divided into two categories: passive SIC (PSIC) and active SIC (ASIC) techniques [20], [21], [33]. ASIC techniques are further divided into two categories: active analogue SIC (AASIC) and active digital SIC (ADSIC) techniques [20], [21], [33]. Currently, a combination of PSIC and ASIC techniques is used to implement SIC in FD radios because one SIC technique cannot achieve the required amount of SIC [34]. The next three sections discuss the three categories of SIC techniques.

### **2.2.1 Passive Self-Interference Cancellation**

PSIC involves suppressing the SI signal in the propagation domain before it reaches the RX chain [21], [33]. A good number of PSIC techniques have been proposed. This section looks at some of these techniques.

#### **2.2.1.1 Antenna Separation**

The earliest form of PSIC is presented in [20],[35],[36]. In this technique, the TX and RX chains use separate antennas, as shown in Figure 2.3. This technique exploits path loss to get the required SIC. High suppression values are achieved with this technique. The authors of [36] achieved 70 dB of PSIC using this technique. However, the distance between the transmit and receive antennas must be sufficiently large for this technique to be effective. In [36], the TX and RX antennas were separated by a distance of 5 m. Therefore, this technique is not suitable for applications where the size of the

device is important, as is the case with most mobile wireless communication devices where a small form factor is desirable.

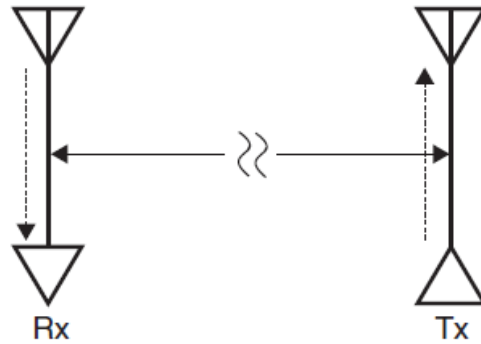


Figure 2.3: PSIC Using Antenna Separation Technique [37].

### 2.2.1.2 Antenna Placement

Antenna placement is another PSIC technique that uses separate antennas to suppress the SI signal [5], [14]. In this technique, one RX antenna is placed between two TX antennas, as shown in Figure 2.4.

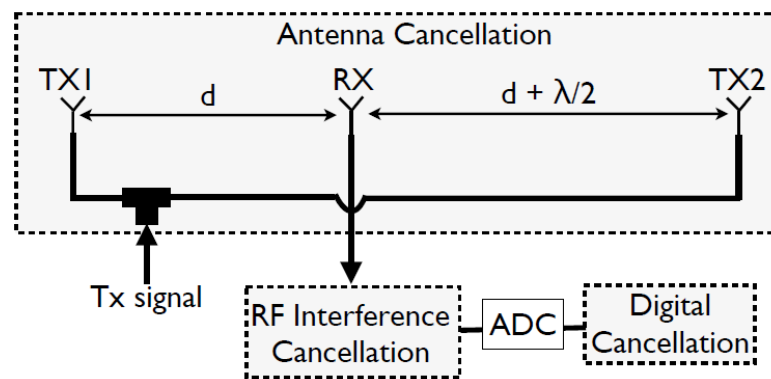


Figure 2.4: PSIC Using Antenna Placement Technique [16].

The RX antenna is placed at a distance  $d$  from one TX antenna and  $d + \lambda/2$  from the other TX antenna, where  $\lambda$  is the wavelength of the carrier frequency. This configuration allows the transmitted signals from the TX antennas to add destructively at the RX antenna, thereby creating a null [14]. The authors of [5] reported a

suppression value of around 30 dB using this technique. However, this technique has the following disadvantages:

1. Three antennas are needed to implement it.
2. It is only effective for narrowband TX signals as its performance degrades with increasing bandwidth [5].

### 2.2.1.3 Directional Antennas

In this technique, the receive antenna is positioned at a point where the transmit antenna's radiation is insignificant [38], [39]. This way, only a small fraction of the transmitted RF signal is coupled to the RX chain [39]. Directional antennas are mainly suited for applications in which directional diversity can be exploited [38]. A radio has directional diversity when the direction in which it transmits is different from the direction in which it receives [38]. Figure 2.5 shows two directional antennas separated by a distance of 50 cm. The authors of [39] reported a suppression value of 45 dB using the antenna configuration shown in Figure 2.5.

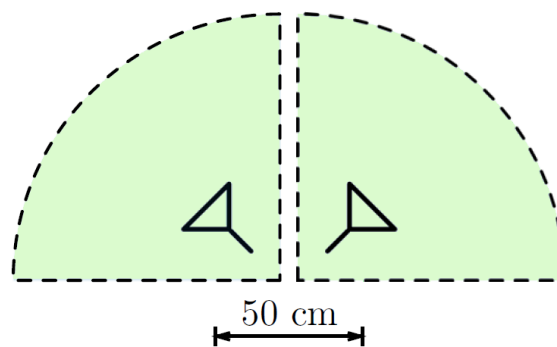


Figure 2.5: Directional Antennas [39].

### 2.2.1.4 Cross Polarisation

Cross polarisation is a PSIC technique in which the TX chain uses a polarisation that is orthogonal to the polarisation used by the RX chain [39], [40]. This technique is applicable to both separate and single antenna FD radios. In separate antenna FD

radios, the TX and RX chains use antennas with orthogonal polarisations, as shown in Figure 2.6. Each antenna in Figure 2.6 is a dual polarised antenna. A slab of RF absorber is placed between the two antennas to increase the isolation between them [39]. The RF absorber used in [38] provided up to 25 dB of absorption. Isolation values of over 70 dB in an anechoic chamber were reported in [38] using the setup shown in Figure 2.6.

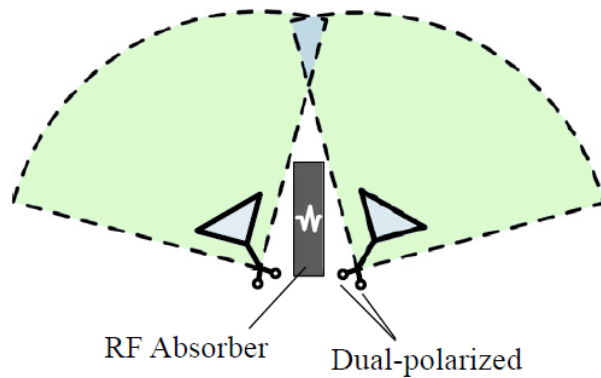


Figure 2.6: Cross Polarisation Using Two Dual Polarised Antennas [39].

Single antenna FD radios that use cross polarisation use antennas that have two ports with orthogonal polarisations, as shown in Figure 2.7 [4]. One port is used to connect the TX chain, and the other port is used to connect the RX chain. Isolation values of over 50 dB were reported in [4] using a dual-polarised antenna.

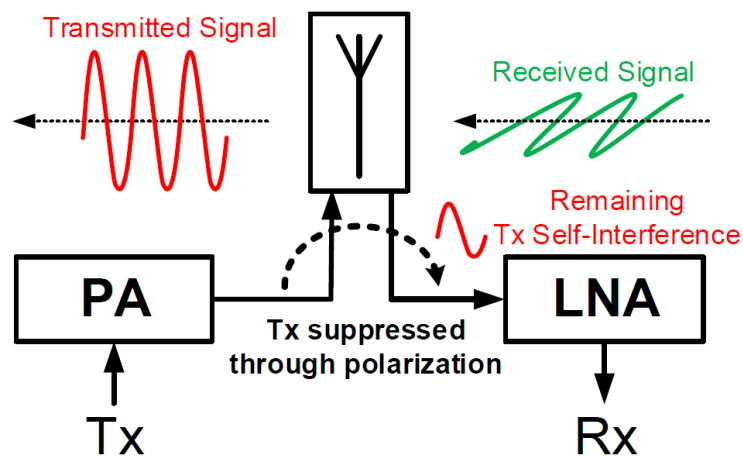


Figure 2.7: Cross Polarisation Using a Dual Polarised Antenna [4].

### 2.2.1.5 Circulator Isolation

In this PSIC technique, a circulator is used to isolate the TX chain from the RX chain in single antenna FD radios, as shown in Figure 2.8. The major disadvantage of this technique is the high power of the SI component that leaks through the circulator and the SI component reflected by the antenna due to impedance mismatch [18], [25]. PSIC techniques that use a circulator in a single antenna configuration are reported in [7] [18], [25], [28], [41]. Circulators provide 20-60 dB isolation between the TX and RX chains [30].

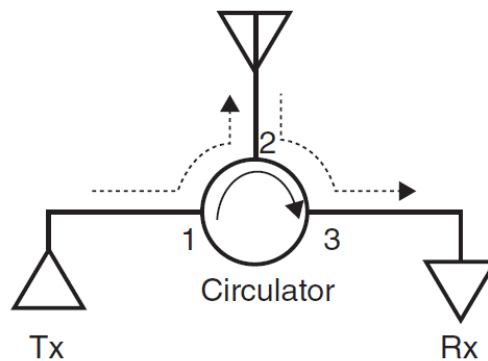


Figure 2.8: PSIC Using a Circulator [37].

### 2.2.1.6 Electrical Balance Duplexer (EBD)

Another technique that is used to isolate the TX chain from the RX chain in a single antenna FD radio is presented in [4], [42], [43]. In this technique, an electrical balance duplexer (EBD) is used as an isolation device. Figure 2.9 shows the operation of an EBD. An EBD consists of a hybrid transformer and a balance network. The EBD balances the antenna impedance with a balance network impedance [43]. It does this by splitting the transmitted RF signal equally between the antenna impedance and the balance network impedance so that no differential voltage excitation occurs [4]. This allows the EBD to pass signals between the TX chain and the antenna, and the RX chain and the antenna while isolating the TX chain from the RX chain [43]. The SIC

technique that uses an EDB presented in [4] achieved 50 dB of isolation over a bandwidth of 6 MHz.

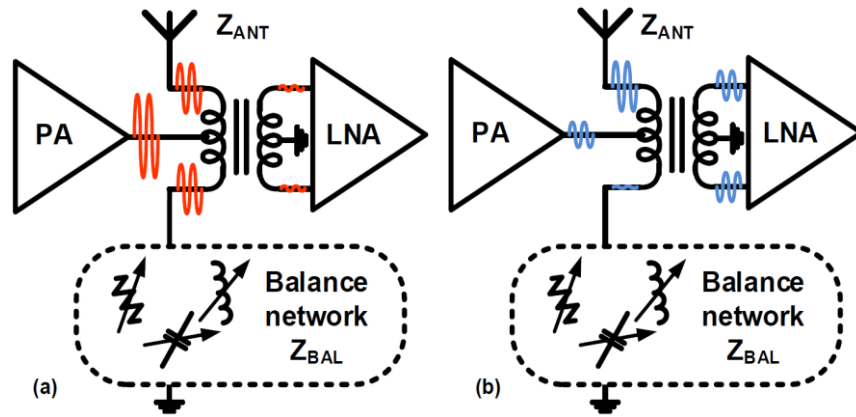


Figure 2.9: EBD Operation: a)Transmission b)Reception [4].

### 2.2.2 Active Analogue Self-Interference Cancellation

AASIC techniques are implemented just after PSIC techniques [14]. They are used to cancel the SI signal before it enters the RX chain [6], [37]. This prevents the saturation of the RX chain. There are two main categories of AASIC techniques [37]:

1. Auxiliary TX chain based AASIC techniques.
2. Tuneable RF circuit based AASIC techniques.

Both categories of AASIC techniques use the same basic idea: a reference signal is tapped from the TX chain, processed and then subtracted from the received signal before it enters the RX chain [6], [37]. The next two sections look at these two categories of AASIC techniques.

#### 2.2.2.1 Auxiliary Transmitter Based AASIC Techniques

In AASIC techniques that use an auxiliary TX chain, the reference signal is tapped from the digital baseband domain of the TX chain and is processed using linear and non-linear pre-distortion signal models to generate a replica of the SI signal [17]. An auxiliary transmitter chain is then used to up-convert the generated replica signal into

the RF domain where AASIC takes place [6]. Figure 2.10 shows an AASIC technique that uses an auxiliary TX chain.

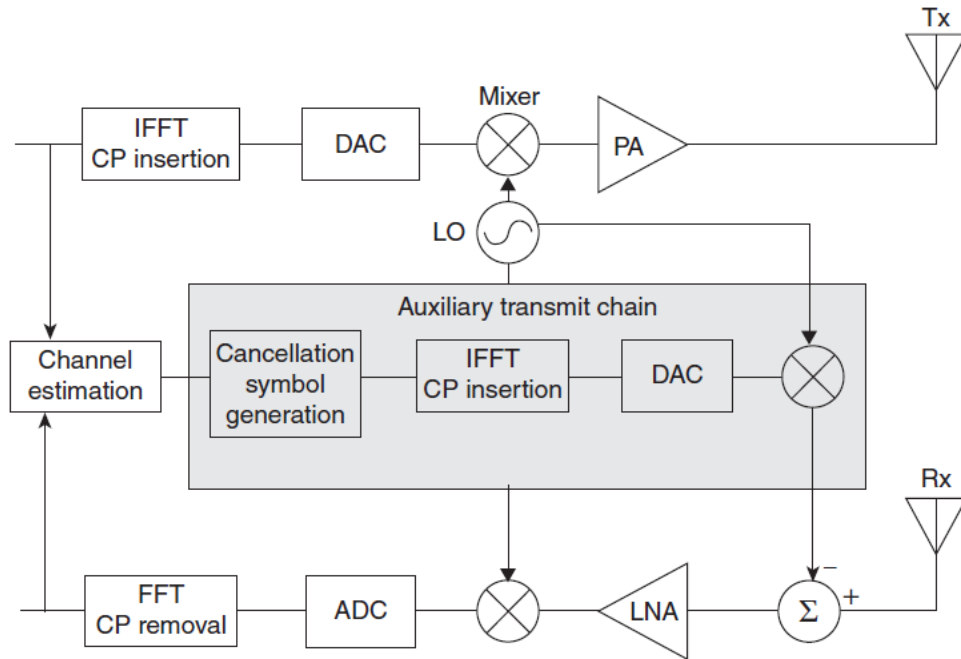


Figure 2.10: AASIC Using an Auxiliary TX Chain [37].

Auxiliary TX chain based AASIC techniques are reported in [17], [35], [44], [45], [46]. The authors of [35], [45], [46] used an auxiliary TX chain in conjunction with two antennas. The authors of [17] used an auxiliary TX chain with a circulator and reported cancellation values in the range of 45-50 dB. In [44], cancellation values of more than 80 dB were reported using an auxiliary TX chain and an EBD. The advantage of techniques that use an auxiliary TX chain is that digital signal processing (DSP) is used to create a replica of the SI signal [47]. However, using an auxiliary TX chain has several disadvantages:

1. The impairments of the TX chain are not accounted for in the reference signal.

Therefore, the performance of the system is highly dependent on how well the

linear and nonlinear distortions in the main TX chain are estimated in the auxiliary TX chain [47].

2. An additional TX chain is required.

### 2.2.2.2 Tuneable RF Circuit Based AASIC Techniques

AASIC techniques that use tuneable RF circuits are the most widely used AASIC techniques [16], [18], [24], [48]. Figure 2.11 shows an AASIC technique that uses a tuneable RF circuit. These techniques are commonly used because tapping the reference signal after the TX chain's power amplifier (PA) ensures that all the TX's linear and nonlinear distortions are included in the reference signal [47]. Therefore, it is not necessary to estimate them separately.

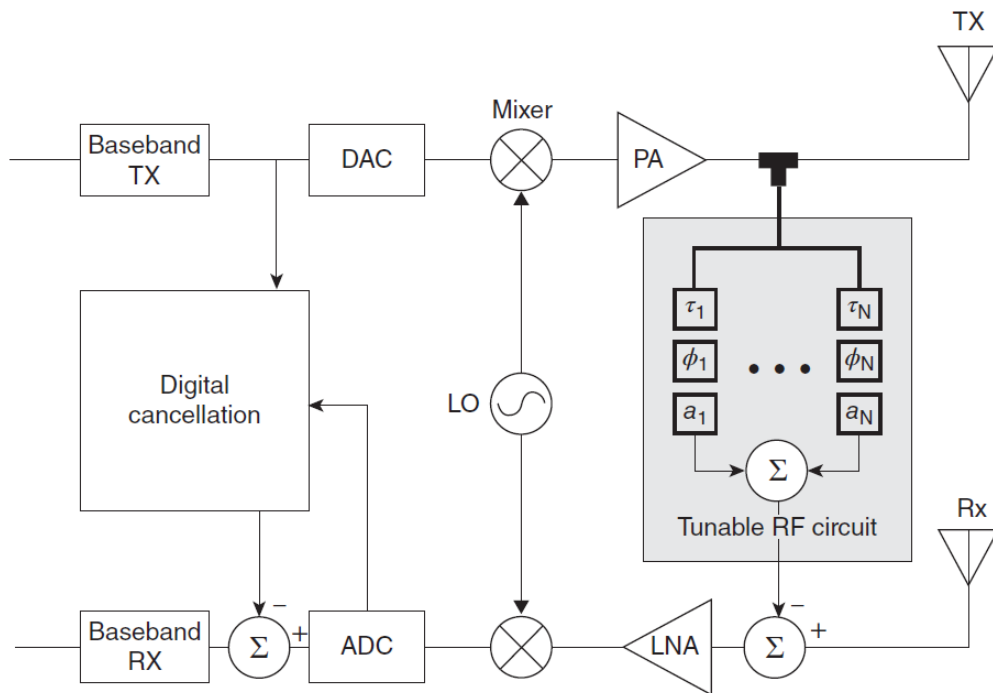


Figure 2.11: AASIC Using a Tuneable RF Circuit [37].

In [18], the authors presented a 16-tap tuneable RF circuit with tuneable attenuators and fixed delays. The circuit was designed to cancel the SI component that leaks through the circulator and the SI component reflected by the antenna due to impedance

mismatch. These two SI components were reported to have average delays of 400 ps and 1.4 ns, respectively. Half of the 16 lines in [18] had delays centred around 400 ps and were tuned to cancel the SI component that leaks through the circulator. The other half were centred around 1.4 ns were tuned to cancel the SI component reflected by the antenna due to impedance mismatch. This design achieved AASIC values of 57 dB and 47 dB over bandwidths of 20 MHz and 80 MHz, respectively.

The authors of [16], on the other hand, used a Balanced/unbalanced (Balun) transformer to tap the reference signal and invert its phase. An attenuator and a time delay were then used to adjust its amplitude and delay. The system achieved 45 dB of AASIC over a bandwidth of 40 MHz.

In [24] and [48], the authors presented AASIC techniques that used a vector modulator (VM) and a tuneable RF circuit with parallel delay taps. The VM was used to adjust the amplitude and phase of the reference signal, while the tuneable RF circuit was used to set its delay. The design in [24] achieved 33 dB of AASIC over a bandwidth of 20MHz. The technique in [48] achieved an AASIC value of 40 dB over a bandwidth of 80 MHz. Using VMs to adjust the amplitude and phase of the reference signal allowed the authors of [24] and [48] to use fewer than the technique in [18].

The major advantage of techniques that use tuneable RF circuits is that the TX chain's linear and nonlinear distortions are already included in the tapped reference signal. Therefore, there is no need to estimate them separately.

### **2.2.3 Active Digital Self-Interference Cancellation**

ADSIC techniques are used to cancel the residual SI signal after the PSIC and AASIC [18], [37]. There are many ways of implementing and categorising ADSIC techniques. In this study, ADSIC techniques are categorised based on the source of the reference

signal. With this form of categorisation, ADSIC techniques can be divided into two main groups:

1. Digital baseband circuit based ADSIC techniques.
2. Auxiliary RX chain based ADSIC techniques.

### 2.2.3.1 Digital Baseband Circuit Based ADSIC Techniques

In ADSIC techniques that use digital baseband circuits, the reference signal is tapped from the digital baseband domain of the TX chain, processed using the channel state information (CSI) and then subtracted from the received signal [14]. Figure 2.12 shows an ADSIC technique that uses a digital baseband circuit. ADSIC techniques that use digital baseband circuits are presented in [49]–[52].

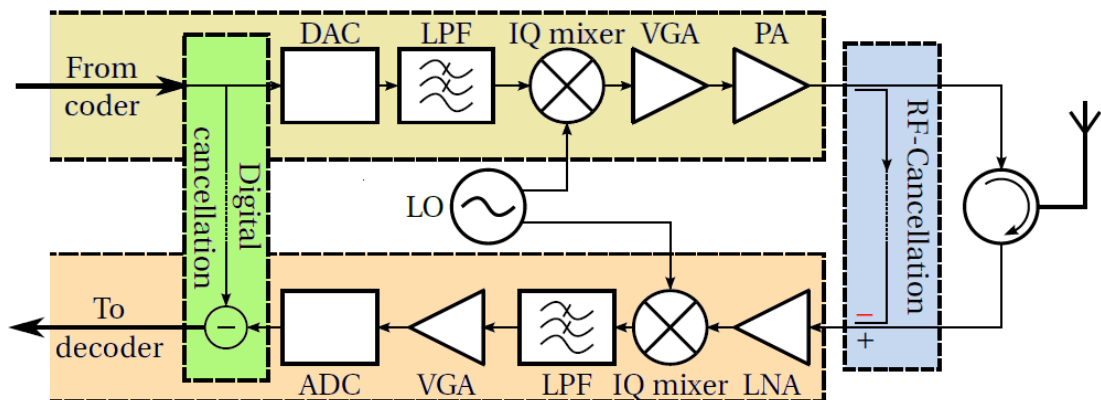


Figure 2.12: ADSIC Using a Digital Baseband Circuit [41].

The authors of [49] proposed a self-adaptive nonlinear digital canceller that used an orthogonalisation procedure for nonlinear basis functions and a parameter learning scheme that used least mean squares (LMS) estimation. In [50], the authors proposed an ADSIC technique that used a Cholesky decomposition-based pre-transmission transformation to enhance the cancelling of nonlinear SI components.

The authors of [51] proposed a low computation ADSIC technique that used Fast Fourier Transform (FFT) processing to generate the SIC signal in the digital domain.

The authors of [52] proposed the use of a variable fractional delay (VFD) finite impulse response (FIR) filter with more precise delay alignment to cancel the residual SI signal in the digital domain.

The main advantage of ADSIC techniques that use digital baseband circuits is that designers can use DSP to create advanced algorithms with relative ease [6]. However, since the signal is tapped in the digital baseband domain, the TX chain's impairments are not included in the tapped signal. Therefore, these impairments have to be estimated separately [47].

### **2.2.3.2 Auxiliary Receiver Chain Based ADSIC Techniques**

In ADSIC techniques that use auxiliary RXs, the reference signal is tapped from the output of the TX chain [2], [33]. It is then attenuated to a suitable level, and an auxiliary RX chain is used to down-convert it to digital baseband. The resulting digital baseband signal is used to get the CSI. The CSI and the digital baseband signal are then used to generate the cancellation signal. The cancellation signal is subtracted from the received signal to cancel the residue SI signal [33]. A typical ADSIC technique that uses an auxiliary RX is shown in Figure 2.13.

Several ADSIC techniques that use an auxiliary RX chain have been proposed in literature [2], [33], [53], [54]. The authors of [2] proposed a two-stage iterative ADSIC technique that aimed to reduce the error in the estimation of the SIC signal introduced by the presence of the SOI in the received signal. The authors of [33] presented a technique that used an auxiliary RX chain in which a common oscillator was used between the auxiliary and ordinary RX chains to mitigate the effects of phase noise. The least-squares (LS) estimation method was used to get the CSI. The authors of [53] proposed a two-stage iterative ADSIC technique based on echo cancellation while in

[54] the use of an auxiliary RX chain was extended to multiple-inputs multiple-outputs (MIMO) systems.

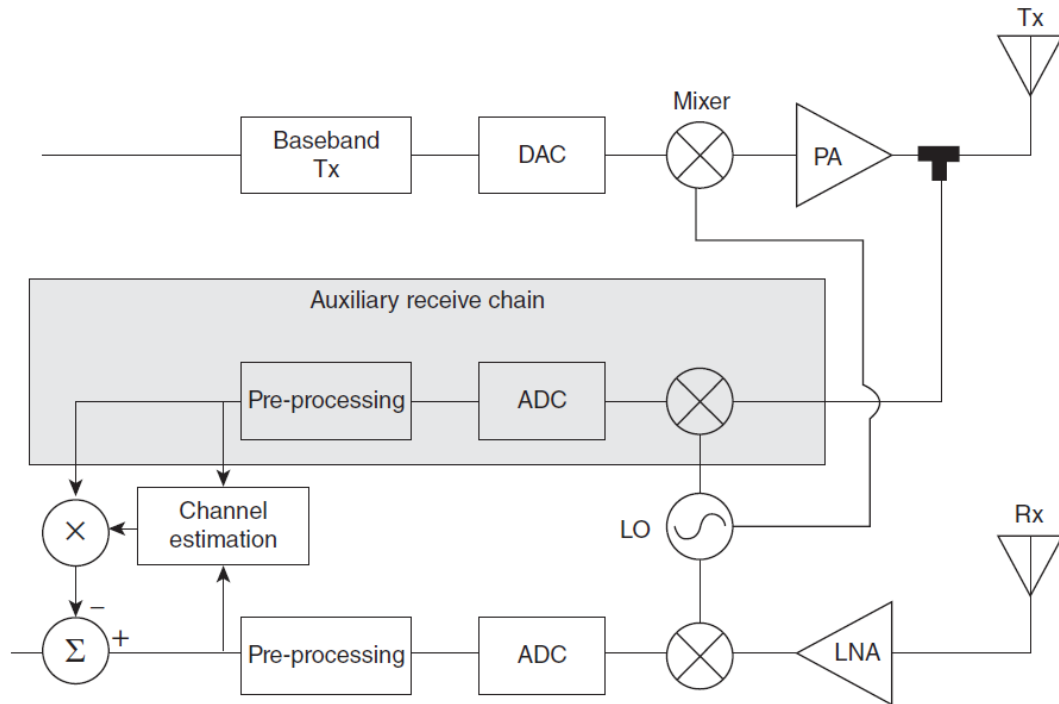


Figure 2.13: ADSIC Using an Auxiliary RX Chain [37].

The main advantage of using an auxiliary RX chain to implement ADSIC is that the TX chain's impairments are included in the tapped reference signal [37]. Therefore, there is no need to estimate them separately. This means that simpler algorithms which require less computational power can be used [47]. However, these types of techniques require the use of an auxiliary RX chain.

#### 2.2.4 Self-Interference Cancellation Summary

SIC techniques are generally divided into two categories: PSIC and ASIC techniques [20], [21], [33]. ASIC techniques are further divided into two categories: AASIC and ADSIC techniques [20], [21], [33]. A combination of techniques is used to implement SIC in FD radios because none of the existing techniques can achieve the required amount of cancellation on their own [34].

In general, PSIC and AASIC techniques are used to suppress the SI signal to a level where it will not saturate the RX chain [6], [37]. ADSIC techniques are used to cancel the residual SI signal after PSIC and AASIC to a level that is equal to/less than the noise floor of the RX chain [6], [37]. Figure 2.14 gives a summary of SIC techniques.

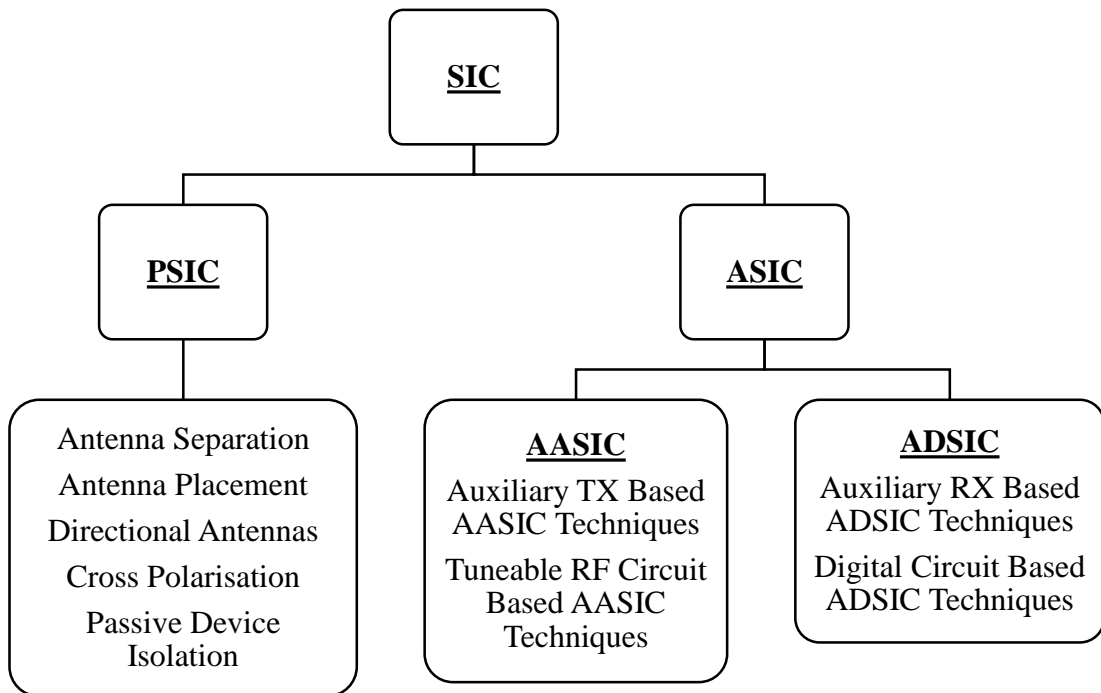


Figure 2.14: Summary of SIC Techniques.

### 2.3 Direct Conversion Receiver

There are three commonly used RX architectures in wireless communication systems. These are the superheterodyne RX, low intermediate frequency (IF) RX and direct conversion RX (DCR) [55], [56]. This study looks at the DCR architecture because it is widely used in most wireless communication systems today due to its simplicity, low power consumption and small form factor [47], [55]. Figure 2.15 shows a block diagram of a typical DCR.

The DCR directly converts the received signal from RF to baseband [47]. The operation of a DCR can be summarised as follows [55]–[60]: The antenna feeds the

received signal into a bandpass filter (BPF) where the desired signal is selected. The selected signal is then amplified by a low noise amplifier (LNA) and down-converted to baseband by an in-phase and quadrature (IQ) mixer. The IQ mixer mixes the selected signal with a signal from a local oscillator (LO) whose frequency is equal to the carrier frequency of the selected signal.

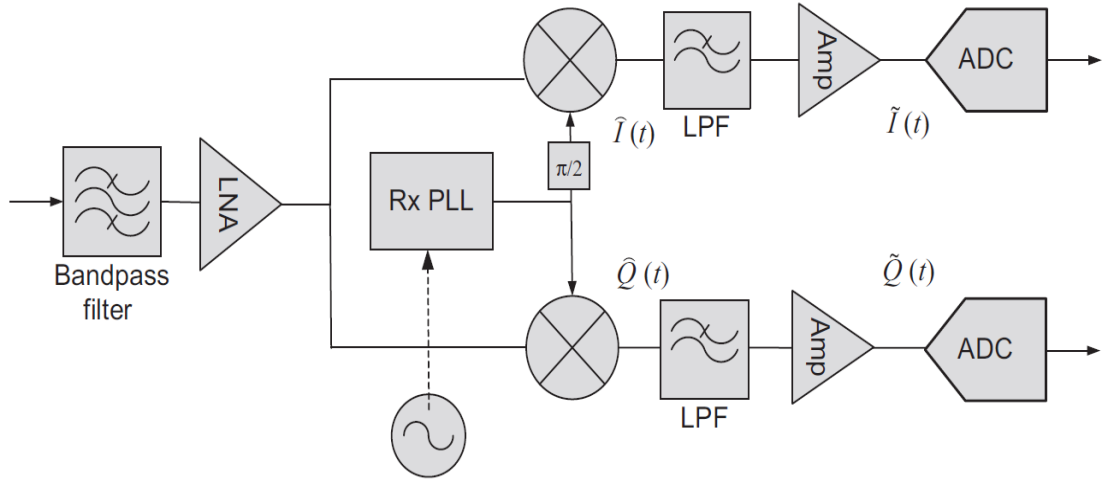


Figure 2.15: Direct Conversion Receiver [55].

The mixing process produces an in-phase (I) component and a quadrature (Q) component. The I and Q components are filtered through lowpass filters (LPFs) and amplified by variable gain amplifiers (VGAs). The VGAs control the signal power, ensuring that the dynamic range of the analogue to digital converters (ADCs) are fully utilised despite the power variation in the received signal. Finally, the ADCs convert the I and Q components into digital.

The received signal after the LNA is given by (8.1) in [55] as:

$$S(t) = I(t) \cos(2\pi f_c t + \theta(t)) + Q(t) \sin(2\pi f_c t + \theta(t)) \quad (2.2)$$

where  $f_c$  is the carrier frequency,  $\theta(t)$  is the general phase difference between the

transmitter and the receiver modulators,  $I(t)$  is the I term and,  $Q(t)$  is the Q term [55]. The amplified received signal  $S(t)$  in (2.2) is down-converted to baseband by mixing it with a signal from the LO to get the I and Q components. The I component is given by (8.2) in [55] as:

$$\begin{aligned}
\hat{I} &= S(t) \cos(2\pi f_c t) \\
&= \cos(2\pi f_c t) [I(t) \cos(2\pi f t + \theta(t)) + Q(t) \sin(2\pi f_c t + \theta(t))] \\
&= I(t) \cos(2\pi f_c t) \cos(2\pi f_c t + \theta(t)) + Q(t) \cos(2\pi f_c t) \sin(2\pi f_c t + \theta(t)) \\
&= \frac{1}{2} I(t) [\cos(\theta(t)) + \cos(4\pi f_c t + \theta(t))] \\
&\quad + \frac{1}{2} Q(t) [\sin(\theta(t)) + \sin(4\pi f_c t + \theta(t))] \tag{2.3}
\end{aligned}$$

Similarly, the Q component is given by (8.3) in [55] as:

$$\begin{aligned}
\hat{Q} &= S(t) \sin(2\pi f_c t) \\
&= \sin(2\pi f_c t) [I(t) \cos(2\pi f_c t + \theta(t)) + Q(t) \sin(2\pi f_c t + \theta(t))] \\
&= I(t) \sin(2\pi f_c t) \cos(2\pi f_c t + \theta(t)) + Q(t) \sin(2\pi f_c t) \sin(2\pi f_c t + \theta(t)) \\
&= \frac{1}{2} I(t) [\sin(\theta(t)) + \sin(4\pi f_c t + \theta(t))] \\
&\quad + \frac{1}{2} Q(t) [\cos(\theta(t)) - \cos(4\pi f_c t + \theta(t))] \tag{2.4}
\end{aligned}$$

Both  $\hat{I}$  and  $\hat{Q}$  pass through LPFs where high-frequency components are removed. After removing the high-frequency components, (2.3) and (2.4) reduce to (2.5) and (2.6), respectively [55].

$$\tilde{I} \approx \frac{1}{2} I(t) \cos(\theta(t)) + \frac{1}{2} Q(t) \sin(\theta(t)) \tag{2.5}$$

$$\tilde{Q} \approx \frac{1}{2} I(t) \sin(\theta(t)) + \frac{1}{2} Q(t) \cos(\theta(t)) \tag{2.6}$$

If  $\theta(t) \approx 0$ , then (2.5) and (2.6) can further be reduced to (2.7) and (2.8), respectively [55].

$$\tilde{I} \approx \frac{1}{2} I(t) \cos(\theta(t)) \quad (2.7)$$

$$\tilde{Q} \approx \frac{1}{2} Q(t) \cos(\theta(t)) \quad (2.8)$$

Equations (2.7) and (2.8) represent the I and Q components at the inputs of the ADCs, respectively, as shown in Figure 2.15.

## CHAPTER 3 : METHODOLOGY

This chapter presents the methodology used to conduct this study. It outlines the methods and materials used to design and simulate the proposed analogue radio frequency (RF) self-interference (SI) canceller.

### 3.1 Signal Model

The signal received at the input of the RX chain of a full-duplex (FD) radio can be expressed as:

$$y(t)_{RX} = y(t)_{SOI} + y(t)_{SI} + n(t) \quad (3.1)$$

where  $y(t)_{SOI}$  is the signal of interest (SOI),  $y(t)_{SI}$  is the SI signal and  $n(t)$  represents noise. The SI signal,  $y(t)_{SI}$ , in (3.1) can be expressed in terms of the transmitted RF signal at the output of the TX chain as:

$$y(t)_{SI} = h(t) * x(t) + \eta(t) \quad (3.2)$$

where  $x(t)$  is the transmitted RF signal at the output of the TX chain,  $h(t)$  is the multipath coupling channel,  $\eta(t)$  represents noise and  $*$  denotes the convolution operation [24].

The SI signal propagates from the TX chain to the RX chain via multiple paths [48].

Therefore, the SI signal given by (3.2) can be expressed as:

$$y(t)_{SI} = \sum_{n=1}^N g_n x(t - \tau_n) + \eta(t) \quad (3.3)$$

where  $g_n$  and  $\tau_n$  are the complex coupling coefficient and delay of the  $n$ th SI component, respectively,  $N$  is the number of SI components and  $\eta(t)$  represents noise [48].

### 3.2 Proposed Analogue RF Self-Interference Canceller

This section presents the proposed analogue RF SI canceller. Figure 3.1 shows the schematic of the canceller. The canceller uses an analogue RF circuit with two taps. Each tap has a tuneable attenuator, delay and phase shifter. The canceller works in conjunction with a circulator, which isolates the TX chain from the RX chain. The circulator was selected because of its simplicity.

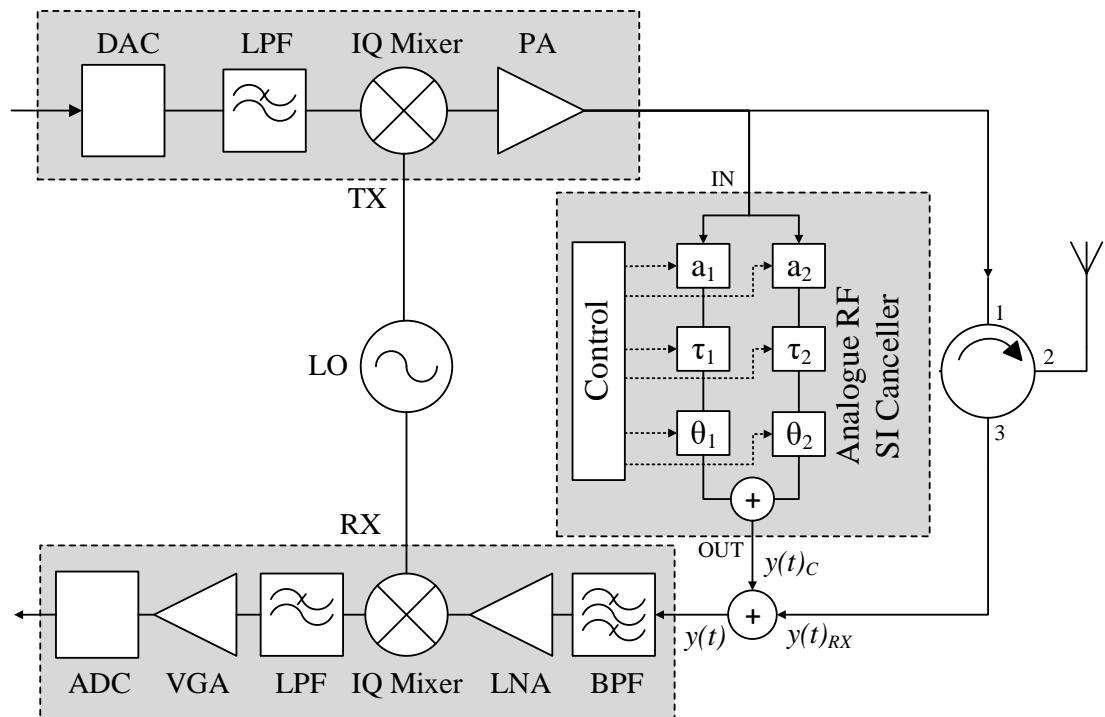


Figure 3.1: Proposed Analogue RF Self-Interference Canceller.

The output of the TX chain is connected to port 1 of the circulator, the antenna is connected to port 2 of the circulator, and the RX chain is connected to port 3 of the circulator. The TX chain feeds the transmitted RF signal into port 1, which routes it to port 2. The antenna feeds the received signal into port 2, which routes it to port 3. The reference signal is tapped from the output of the TX chain and fed into the analogue RF SI canceller to generate the cancellation signal. The reference signal contains all the impairments of the TX chain since it is tapped from the output of the TX chain

[47]. Therefore, it is not necessary to include these impairments in the signal model. The cancellation signal is combined with the received signal on port 3 of the circulator to cancel the SI signal.

Equation (2.1) shows that the SI signal in a single antenna FD radio that uses a circulator to isolate the TX chain from the RX chain has three components:

1. The SI component that leaks through the circulator.
2. The SI component reflected by the antenna.
3. The NLOS SI component reflected from the environment.

Therefore, for a single antenna FD radio that uses a circulator to isolate the TX chain from the RX chain, the SI signal given by (3.3) can be expressed as:

$$y(t)_{SI} = g_C x(t - \tau_C) + g_A x(t - \tau_A) + \sum_{k=1}^K g_k x(t - \tau_k) + \eta(t) \quad (3.4)$$

where  $g_C$  and  $\tau_C$  are the complex coupling coefficient and delay of the SI component that leaks through the circulator, respectively;  $g_A$  and  $\tau_A$  are the complex coupling coefficient and delay of the SI component reflected by the antenna, respectively;  $g_k$  and  $\tau_k$  are the complex coupling coefficient and delay of the  $k$ th SI component reflected from the environment, respectively;  $K$  is the number of SI components reflected from the environment; and  $\eta(t)$  represents noise. The first two terms in (3.4) have significantly more power than the summation term [24], [25]. In addition, the characteristics of these two terms are constant since they depend on the structure of the radio, while those of the summation term vary with the environment [6].

The strategy in this study was to use the analogue RF SI canceller to cancel the first two terms in (3.4). A similar strategy was used in [18]. However, the analogue RF SI canceller used in [18] had 16 taps, while the canceller proposed in this study has two taps, as shown in Figure 3.1. Each tap consists of a tuneable attenuator, delay, and phase shifter. The ability to tune all the three parameters enables the proposed canceller to use fewer taps than the canceller presented in [18].

The design of the analogue RF SI canceller was based on the following insight: the SI components represented by the first two terms in (3.4) can be cancelled in the analogue domain because their characteristics are constant [6]. This is done by combining the received signal with the cancellation signal. The cancellation signal is generated by taking the reference signal from the output of the TX chain and feeding it into the analogue RF SI canceller where it is modified using estimates of the attenuation, delay and phase of the two SI components.

The estimates of the attenuation, delay and phase used to generate the cancellation signal are obtained by tuning the attenuators, delays and phase shifters of the analogue RF SI canceller shown in Figure 3.1. The first tap of the canceller is tuned to cancel the SI component that leaks through the circulator; while the second tap is tuned to cancel the SI component reflected by the antenna. The resulting signal after cancellation will not saturate the RX chain because the SI components represented by the first two terms in (3.4) account for the majority of the power of the SI signal [24], [25].

The output of the analogue RF SI canceller in Figure 3.1 can be expressed as:

$$y(t)_c = -(g_1x(t - \tau_1) + g_2x(t - \tau_2)) \quad (3.5)$$

where  $x(t)$  is the transmitted RF signal at the output of the TX chain;  $g_1$  is the complex-valued coefficient modelling the attenuation,  $a_1$ , and phase,  $\theta_1$ , of the first tap of the canceller;  $\tau_1$  is the delay of the first tap of canceller;  $g_2$  is the complex-valued coefficient modelling the attenuation,  $a_2$ , and phase,  $\theta_2$ , of the second tap of the canceller; and  $\tau_2$  is the delay of the second tap of the canceller.

The signal after cancellation in Figure 3.1 can then be expressed as:

$$y(t) = y(t)_{RX} + y(t)_C$$

$$y(t) = y(t)_{RX} - (g_1x(t - \tau_1) + g_2x(t - \tau_2)) \quad (3.6)$$

The values of  $g_1$ ,  $\tau_1$ ,  $g_2$  and  $\tau_2$  in (3.5) and (3.6) are obtained by tuning the attenuators, delays and phase shifters of the two taps of the canceller shown in Figure 3.1. The tuning process seeks to minimise the SI signal after AASIC:

$$\min[y(t)_{RX} - (g_1x(t - \tau_1) + g_2x(t - \tau_2))]^2 \quad (3.7)$$

Note that the canceller does not alter the SOI because the SOI and  $x(t - \tau_n)$  are uncorrelated [7]. Therefore, the minimum value of (3.7) gives the optimal values of  $g_1$ ,  $\tau_1$ ,  $g_2$  and  $\tau_2$ .

### 3.3 System Simulation

This section presents the simulation of the proposed analogue RF SI canceller. The simulation was done in MATLAB R2018a using Simulink 9.1. The model was created using function blocks from four Simulink block libraries, namely: Simulink, Communications System Toolbox, DSP System Toolbox and RF Blockset. The Appendix gives the configurations of the function blocks used in the simulation.

The model shown in Figure 3.2 was used to simulate the proposed SI canceller in MATLAB/Simulink. The model was divided into four main parts:

1. SOI Source.
2. SI Source.
3. Circulator.
4. Analogue RF SI Canceller.

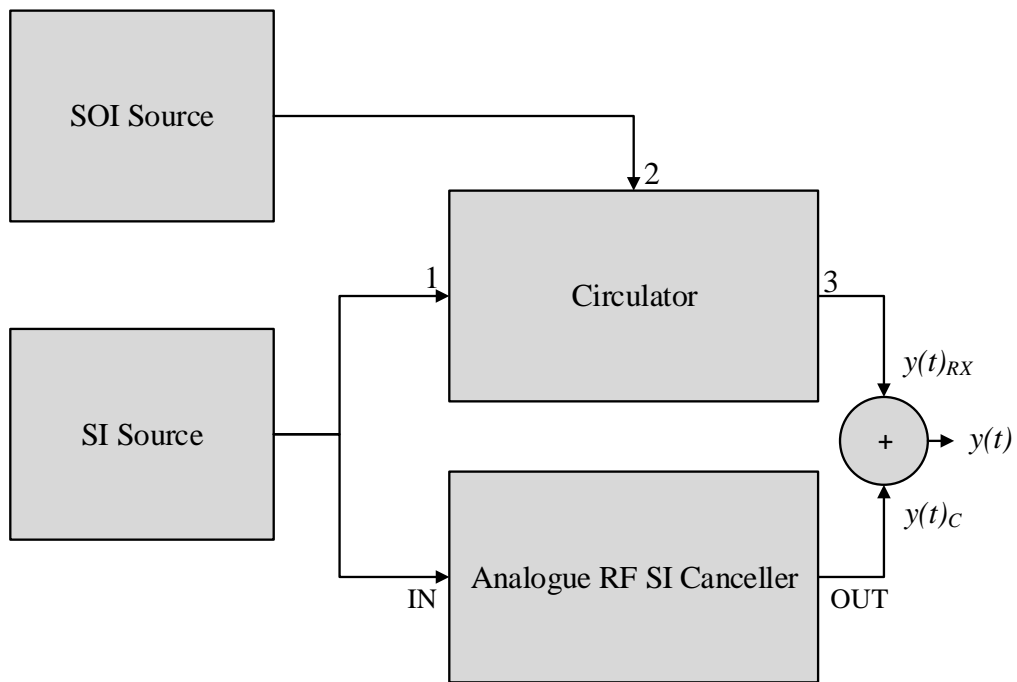


Figure 3.2: Model Used in System Simulation.

In the system simulation, an FD radio operating at 2.45 GHz with a bandwidth of 20 MHz was considered. Two test signals were used to analyse the performance of the proposed design. No coding was applied to the signals for simplicity. The first signal was assigned as the SI signal. The data of this signal was generated using a Bernoulli Binary Generator and modulated using binary phase-shift keying (BPSK). The output samples of the BPSK modulator were processed through a square root cosine raised filter. The resulting signal was up-converted to 2.45 GHz and amplified using a power

amplifier (PA). The output power of the signal was set to 20 dBm. Figure 3.3 shows the SI source model used to generate the SI signal in MATLAB/Simulink.

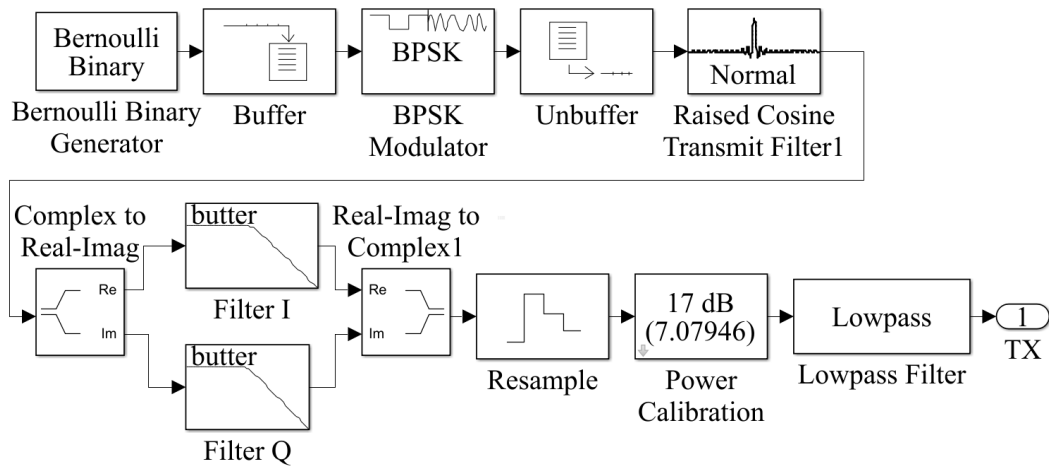


Figure 3.3: SI Source Model.

The second signal was assigned as the SOI. The data of this signal was generated by combining level-shifted data from a Bernoulli Binary Generator and a Pseudo-Noise Sequence Generator. The resulting data was modulated using offset quadrature phase-shift keying (OQPSK). The signal was then up-converted to 2.45 GHz and amplified using a PA. The output power of the signal was set to -50 dBm. Figure 3.4 shows the SOI source model used to generate SOI in MATLAB/Simulink.

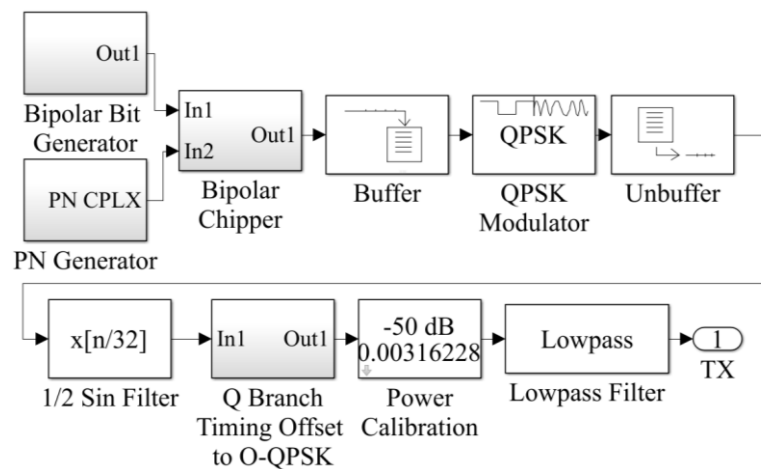


Figure 3.4: SOI Source Model.

The RF SI signal and SOI were then fed into the circulator. Figure 3.5 shows the model used to simulate the circulator in MATLAB/Simulink. The model had signal paths to simulate:

1. The SI component that leaks through the circulator.
2. The SI component reflected by the antenna.
3. The NLOS SI component reflected from the environment.

The signal that leaks through the circulator and the signal reflected by the antenna are just attenuated delayed versions of the transmitted RF signal. They were modelled using an attenuator and delay, as shown in Figure 3.6. The SI component reflected from the environment, on the other hand, was modelled using a four path Rayleigh fading channel, as shown in Figure 3.7. This was done under the assumption that there was no dominant signal path among the multipath reflections. The circulator model in Figure 3.5 combined the three SI signal components and the SOI signal to form the received signal.

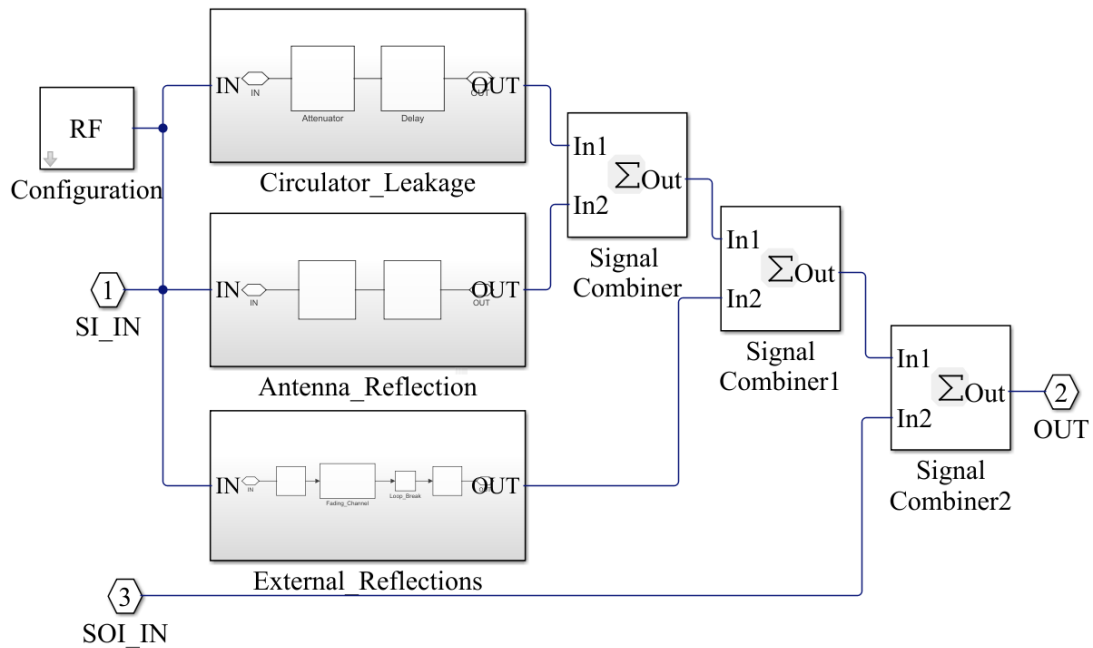


Figure 3.5: Circulator Model.

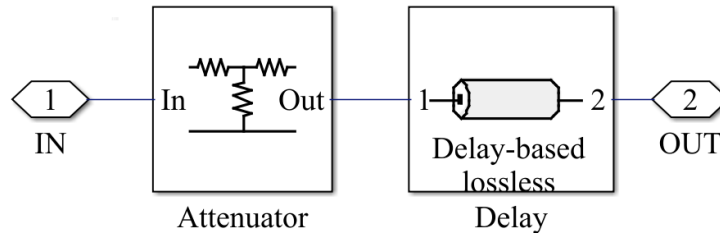


Figure 3.6: Attenuator and Delay Model.

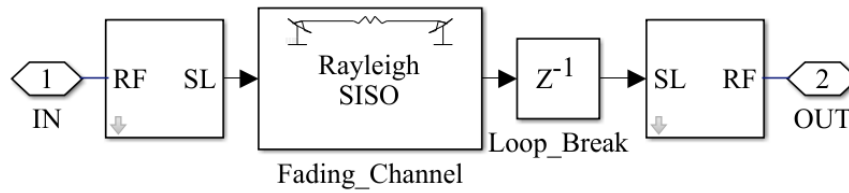


Figure 3.7: Rayleigh Fading Channel Model.

Figure 3.8 shows the model that was used to simulate the analogue RF SI canceller. The model had two signal paths, which were configured to cancel the SI component that leaks through the circulator and the SI component reflected by the antenna. These SI components are represented by the first two terms in (3.4). Each path was implemented using a tuneable attenuator, delay and phase shifter, as shown in Figure 3.9. The attenuator, delay and phase shifter in each signal path were tuned to get the optimal output of the canceller.

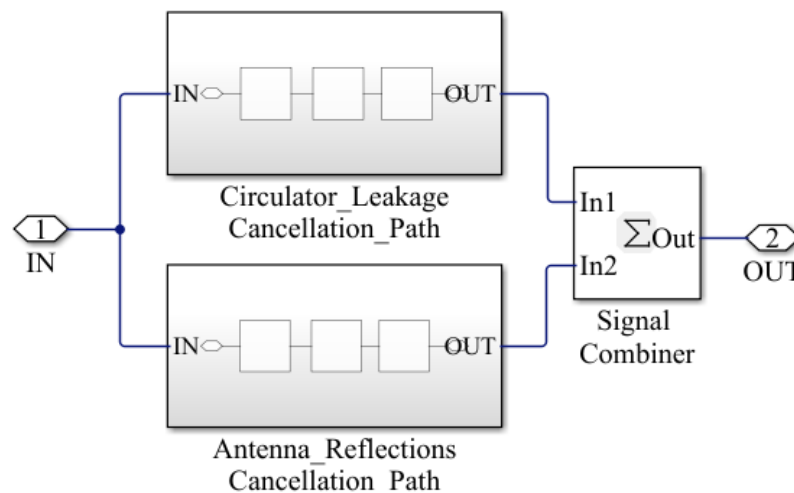


Figure 3.8: Analogue RF SI Canceller Model.

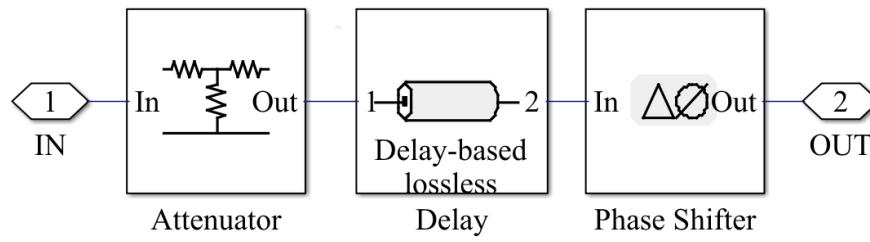


Figure 3.9: Analogue RF SI Canceller Signal Path Model.

The output of the circulator and the output of the analogue RF SI canceller were then combined to cancel the SI signal.

## CHAPTER 4 : RESULTS AND DISCUSSION

This chapter presents the results of the study. Section 4.1 presents the results of the self-interference cancellation (SIC) performance of the proposed analogue RF self-interference (SI) canceller. Section 4.2 compares the SIC performance of the proposed canceller with the SIC performance of alternative designs.

### 4.1 Self-Interference Cancellation Performance

This section presents the results of the SIC performance of the proposed analogue RF SI canceller. The SIC performance consisted of passive SIC (PSIC) and active analogue SIC (AASIC). The circulator provided PSIC; the analogue RF circuit provided AASIC. All signals in this section are represented in complex baseband form. The analysis of the SIC performance of the proposed canceller was performed in two parts. The first part looked at the SIC performance of the proposed canceller in the absence of the SOI, while the second part looked at the SIC performance of the proposed canceller in the presence of the SOI.

#### 4.1.1 Self-Interference Cancellation in the Absence of the Signal of Interest

The model shown in Figure 3.2 was used to analyse the SIC performance of the proposed canceller in the absence of the SOI. However, in this part, the simulation did not include SOI source. Figure 4.1 shows the spectrum of the SI signal generated by the SI source. This signal was fed into port 1 of the circulator model to analyse the SIC performance of the circulator in the absence of the SOI.

Figure 4.2 shows the SIC performance of the circulator in the absence of the SOI. The black spectrum is the SI signal before PSIC at port 1 of the circulator model. The power of this signal was 20 dBm. The blue spectrum is the the SI signal after PSIC at port 3 of the circulator model. This signal is a sum of the three SI components in a single

antenna FD radio that uses a circulator given by (2.1) and noise. The power of this signal was -4 dBm.

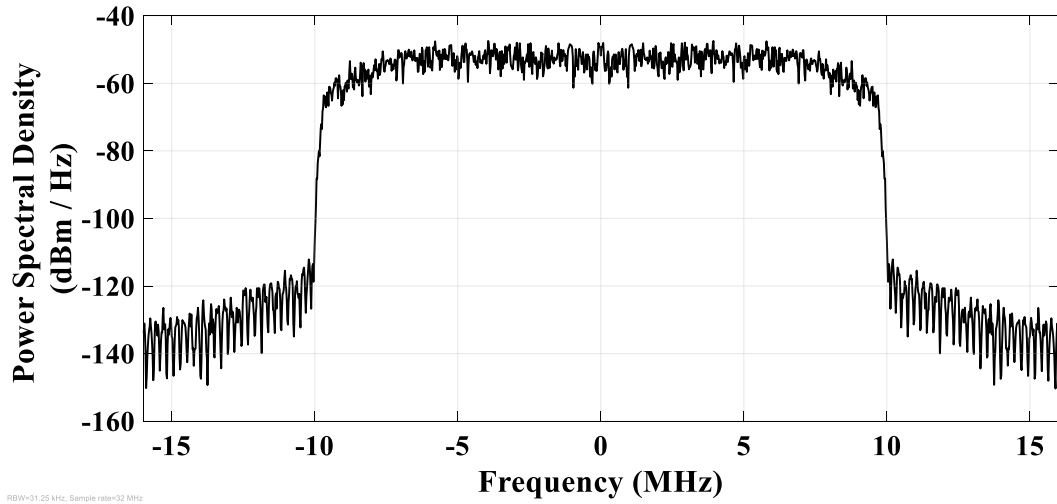


Figure 4.1: Input SI Signal.

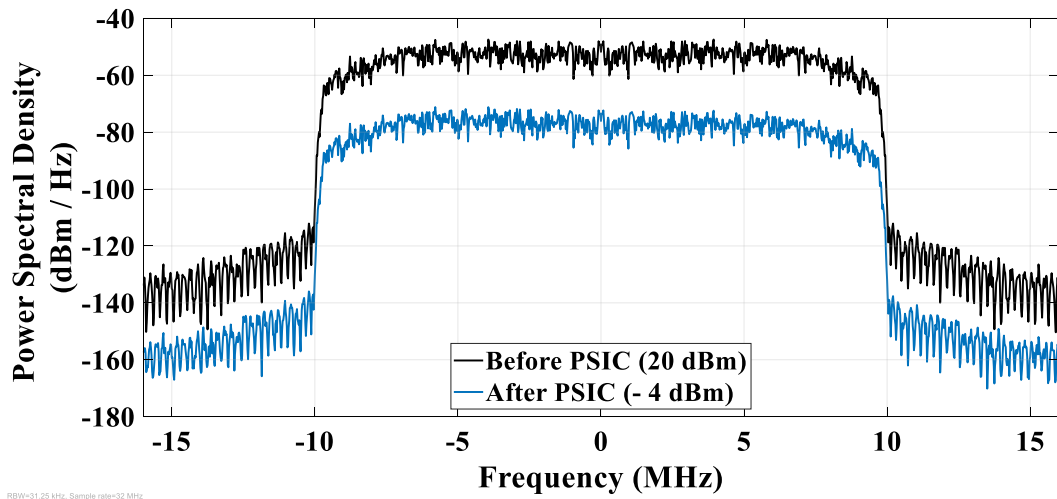


Figure 4.2: PSIC Performance in the Absence of the SOI.

The two signals in Figure 4.2 have similar frequency spectra, but different power. This is because the two signals have similar frequency components as the PSIC technique used in this study isolates the TX chain from the RX chain by suppressing the transmitted RF signal that reaches the RX chain. No new frequency components are added to or removed from the signal in the process.

The SIC performance of the analogue RF SI canceller in the absence of the SOI is shown in Figure 4.3. The blue spectrum is the SI signal before AASIC at port 3 of the circulator model. The red spectrum is the SI signal after AASIC. This signal was obtained by combining the SI signal at port 3 of the circulator model with output of the analogue RF SI canceller model.

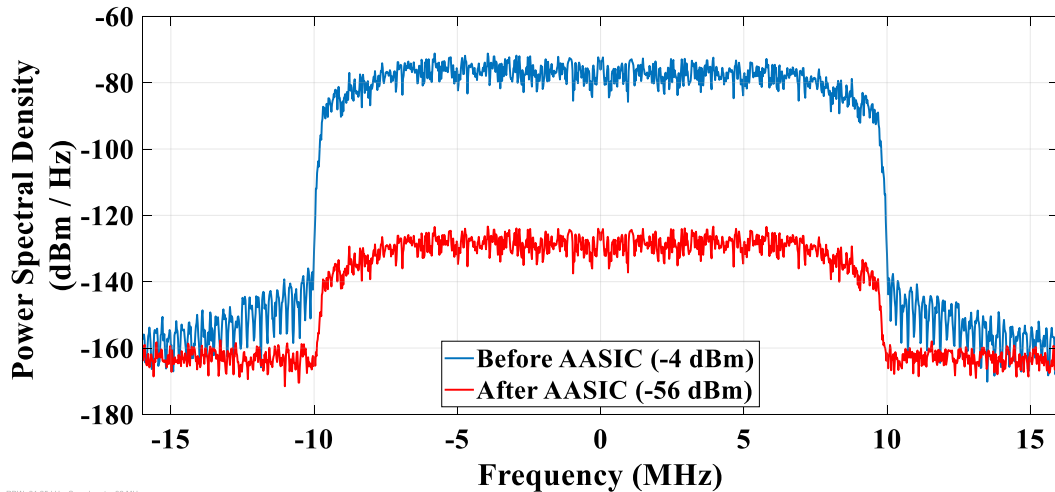


Figure 4.3: AASIC Performance in the Absence of the SOI.

The power of the SI signal after AASIC was measured to be around -56 dBm. This represents 52 dB of AASIC. This is a promising result given the low complexity of the proposed canceller and that the process of tuning the canceller was not yet optimised. At around -56 dBm, the SI signal is at a power level where it would not saturate the RX chain. Table 4.1 summarises the SIC performance of the proposed canceller in the absence of the SOI.

Table 4.1: SIC Performance Summary in the Absence of the SOI.

Description	Value
Input SI signal Power	20 dBm
SI Signal Power After PSIC	-4 dBm
SI Signal Power After AASIC	-56 dBm

#### 4.1.2 Self-Interference Cancellation in the Presence of the Signal of Interest

The SIC performance of the proposed canceller in the presence of the SOI was analysed using the model shown in Figure 3.2. Figure 4.4 shows the SI signal and SOI generated by the SI source and SOI source models, respectively. The power of the SI signal was 20 dBm, while the power of the SOI was -50dBm. The two signals were fed into the circulator model to analyse the SIC performance of the circulator in the presence of the SOI.

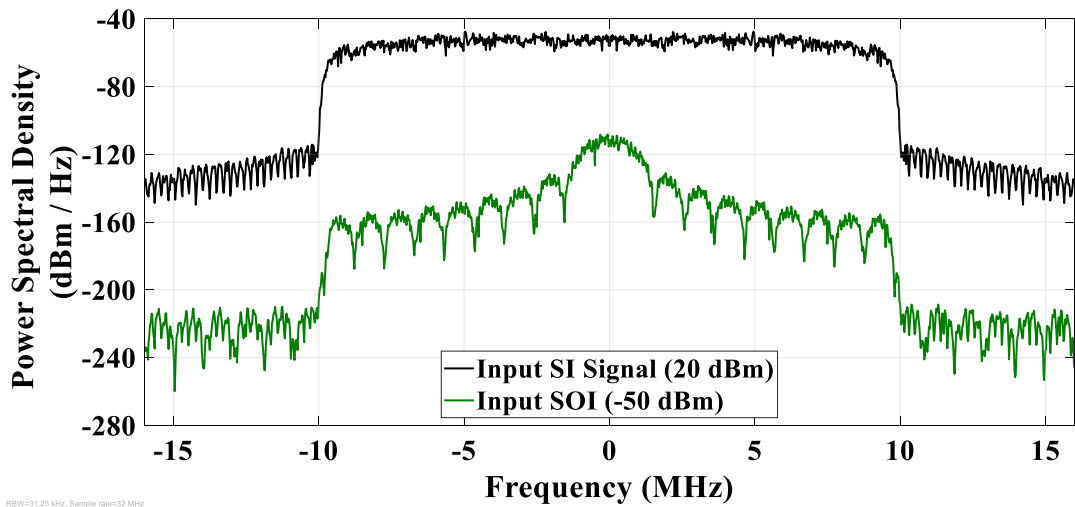


Figure 4.4: Input SI signal and SOI.

Figure 4.5 shows the SIC performance of the circulator in the presence of the SOI. The black spectrum is the SI signal before PSIC at port 1 of the circulator model. The power of this signal was 20 dBm. The blue spectrum is the received signal after PSIC at port 3 of the circulator model. The received signal is a sum of the SI signal, the SOI and noise. The power of this signal was measured to be around -4 dBm. This value is equal to the power of the SI signal after PSIC in Figure 4.2. The spectrum of the received signal after PSIC in Figure 4.5 is also similar to the spectrum of the SI signal after PSIC in Figure 4.2. This is because the SI signal is the dominant signal in the received

signal before AASIC. At this stage, it is very difficult for the RX to recover the SOI from the received signal without further SIC.

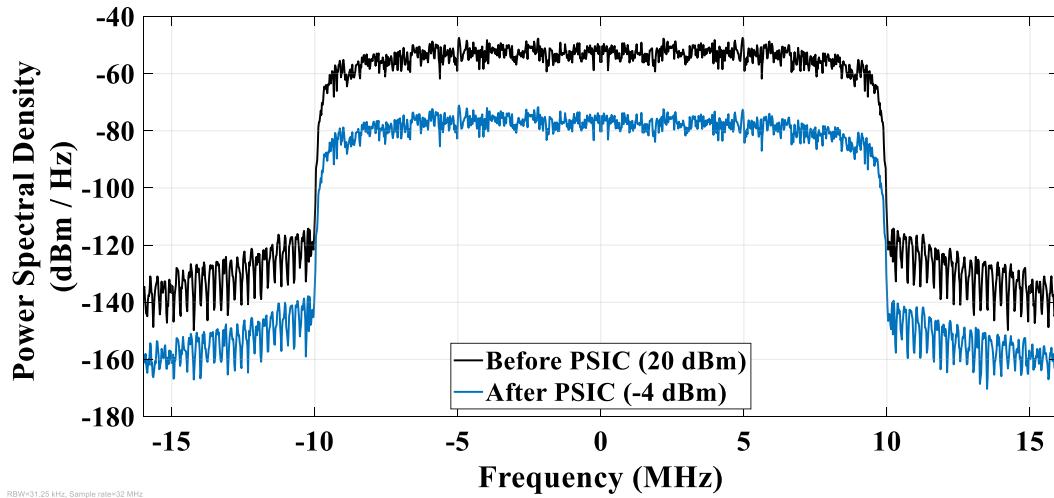


Figure 4.5: PSIC Performance in the Presence of the SOI.

The SIC performance of the analogue RF SI canceller in the presence of the SOI is shown in Figure 4.6. The blue spectrum is the received signal before AASIC at port 3 of the circulator model. The red spectrum is the received signal after AASIC. This signal was obtained by combining the received signal at port 3 of the circulator model with the output of the analogue RF SI canceller model.

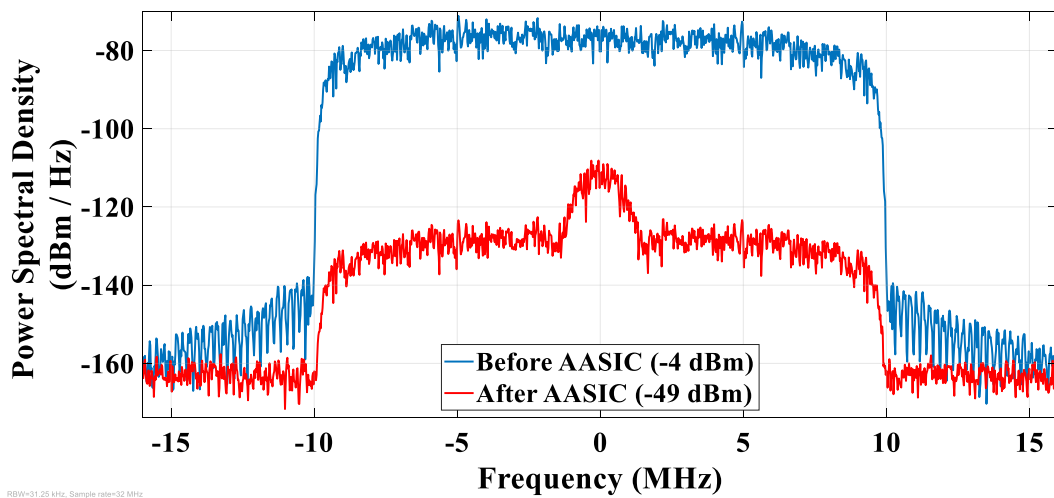


Figure 4.6: AASIC Performance in the Presence of the SOI.

After AASIC, the SI signal is no longer the dominant signal in the received signal. This is clear from Figure 4.6 in which the contribution of the SOI to the received signal is evident. The power of the received signal after AASIC was measured to be around -49 dBm. This value is higher than the power of the SI signal after AASIC found in section 4.1.1. This is because the received signal after AASIC is a sum of the SI signal and SOI. However, a comparison of the spectrum of the received signal after AASIC in Figure 4.6 to the spectrum of the SI signal after AASIC in Figure 4.3 shows that the SIC performance of the canceller in the presence of the SOI is similar to the SIC performance of the canceller in the absence of the SOI.

Furthermore, the shape of the received signal after AASIC in Figure 4.6 shows that the proposed canceller does not alter the SOI. This is demonstrated by Figure 4.7 in which the SOI is superimposed on the received signal after AASIC. Figure 4.7 clearly shows that the SOI is not affected by the proposed canceller. This is line with observations made in [7] that a linear combination of different delayed versions of the SI signal cannot cancel the SOI because the two signals are uncorrelated.

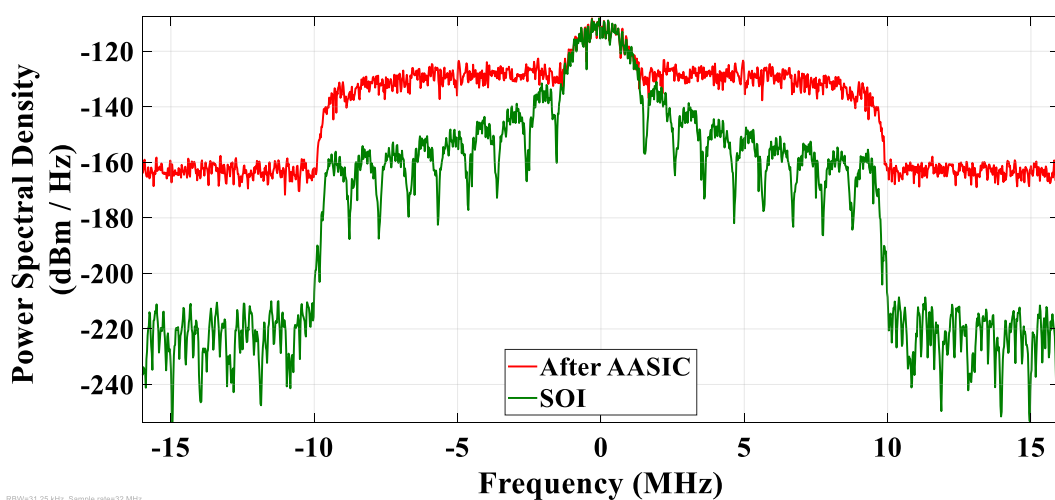


Figure 4.7: Superimposition of SOI on Received Signal After AASIC.

Table 4.2 summarises the SIC performance of the proposed canceller in the presence of the SOI.

Table 4.2: SIC Performance Summary in the Presence of the SOI.

<b>Description</b>	<b>Value</b>
Input SI signal Power	20 dBm
Input SOI Power	-50 dBm
Received Signal Power After PSIC	-4 dBm
Received Signal Power After AASIC	-49 dBm

#### **4.2 Self-Interference Cancellation Performance Comparison**

This section briefly compares the SIC performance of the proposed canceller with the SIC performance of other canceller designs. In studies where a combination of SIC techniques is presented, only the SIC performance of the analogue RF SI canceller is considered.

The authors of [5] presented an AASIC technique that used a QHx220 noise cancelling chip, two transmit antennas and one receive antenna. The design separated the two transmit antennas by a distance of  $d$  and  $d+\lambda/2$  away from the receive antenna. The system provided 20 dB of AASIC over a bandwidth of 15 MHz. However, the combination of passive and active analogue SIC techniques used in [5] is only suitable for narrowband signals as the performance of the system degrades with increasing bandwidth.

In [16], the authors presented a canceller that used an analogue RF circuit, a Balun and separate antennas to cancel the SI signal in the analogue domain. The analogue RF circuit had one tap which consisted of a tuneable attenuator and delay. The system

achieved 45 dB of AASIC over a bandwidth of 40 MHz. However, the authors only considered the line of sight (LOS) SI component when analysing the SIC performance of the system.

The authors of [17] proposed a canceller that used an auxiliary TX chain and separate antennas to cancel the SI signal. The system had a 20 MHz bandwidth and achieved 28 dB of AASIC. In [18], a canceller that used an analogue RF circuit with 16 taps was proposed to cancel the SI signal in analogue RF domain. Each tap had a tuneable attenuator and a fixed delay. The system achieved 57 dB of AASIC over a bandwidth of 20 MHz and 47 dB over a bandwidth of 80 MHz. The main drawback of the canceller in [18] is that a lot of taps are required to implement it.

The authors of [19] proposed a technique that used a vector modulator (VM) and an analogue RF circuit with a fixed delay to cancel the SI signal in the analogue domain. This technique achieved an AASIC value of 36 dB over a bandwidth of 20 MHz. The main disadvantage of this AASIC technique is that the fixed delay has to be carefully set for the system to remove the intended SI components.

The author of [34] proposed a digitally assisted analogue RF canceller. The canceller used an RF vector multiplier in conjunction with a digital rational function finite impulse response (FIR) filter to generate the signal used to cancel the SI signal in analogue RF domain. The system achieved 50 dB of AASIC over a bandwidth of 20 MHz and 40 dB over a bandwidth of 120 MHz channel. However, the author only considered the SI component that leaks through the circulator in a single antenna FD radio when analysing the SIC performance of the canceller.

The analogue RF SI canceller proposed in this study achieves 52 dB of AASIC over a bandwidth of 20 MHz using an analogue RF circuit with two taps. Each tap has a

tuneable attenuation, delay and phase. The ability to tune the attenuation, delay and phase of each tap allows the proposed canceller to use a simple design. Table 4.3 summarises the SIC performance comparison.

Table 4.3: Performance Comparison Summary.

<b>Study</b>	<b>Description</b>	<b>Bandwidth</b>	<b>AASIC</b>
[5]	QHx220 noise cancelling chip, two transmit antennas and one receive antenna.	15 MHz	20 dB
[16]	One tap analogue RF Circuit with Balun Inversion	40 MHz	45 dB
[17]	Auxiliary TX Chain	20 MHz	28 dB
[18]	16 tap analogue RF circuit with tuneable attenuation and fixed delay.	20 MHz 80 MHz	57 dB 47 dB
[19]	VM and one tap analogue RF circuit with fixed delay	20 MHz	36 dB
[34]	VM and rational function FIR filter	20 MHz 120 MHz	50 dB 40 dB
This Work	2 tap analogue RF circuit with tuneable attenuation, phase and delay.	20 MHz	52 dB

## CHAPTER 5 : CONCLUSION AND RECOMMENDATIONS

This chapter presents the conclusion and recommendations of the study. Section 5.1 presents the conclusion, while section 5.2 presents the recommendations.

### 5.1 Conclusion

The main challenge in implementing full-duplex (FD) radios is the self-interference (SI) signal that leaks from the transmitter (TX) chain into the receiver (RX) chain. The literature review in Chapter 2 revealed that a large amount of self-interference cancellation (SIC) before the RX chain is essential for the operation of FD radios. This cancellation aims to prevent the saturation of the RX chain.

This study has proposed an analogue RF SI canceller that cancels the SI signal before it enters the RX chain. The proposed canceller uses an analogue RF circuit with tuneable attenuation, delay and phase to cancel the SI signal. The ability to tune the attenuation, delay and phase of the analogue RF circuit allows the canceller to use a simple design. The canceller works in conjunction with a circulator.

The analysis of the SIC performance of the proposed canceller in the absence of the signal of interest (SOI) shows that the proposed canceller provides sufficient SIC before the RX chain. The proposed canceller achieves 52 dB of AASIC over a bandwidth of 20 MHz. Furthermore, the analysis of the SIC performance of the proposed canceller in the presence of the SOI shows that the proposed canceller cancels the SI signal without affecting the SOI.

The SIC performance of the proposed analogue RF SI canceller was compared with the SIC performance of other canceller designs. It was found that the SIC performance of the proposed canceller is better than the SIC performance of the majority of the

cancellers considered in the comparison. In the SIC performance comparison, the canceller in [5] had the worst SIC performance. It achieved 20 dB of AASIC over a bandwidth of 15 MHz. On the other hand, the canceller in [18] had the best SIC performance. It achieved 57 dB of AASIC over a bandwidth of 20 MHz. Table 4.3 summarises the SIC performance comparison.

## **5.2 Recommendations and Future Work**

In this study, the tuning of the analogue RF circuit was done manually, which affected the SIC performance of the canceller. It is recommended that a self-adaptive algorithm be used to tune the analogue RF circuit. This will improve the performance of the canceller as the tuning algorithm can be easily optimised.

The SIC performance of the proposed analogue RF SI canceller was entirely analysed using software simulations. Therefore, there is a need to analyse the performance of the proposed design using hardware in future work. The study should look at the fabrication of a demonstration board for the analogue RF SI canceller and interfacing it with a circulator and appropriate signal sources.

## REFERENCES

- [1] A. Sabharwal, P. Schniter, D. Guo, D. W. Bliss, S. Rangarajan, and R. Wichman, “In-Band Full-Duplex Wireless: Challenges and Opportunities,” *IEEE J. Sel. Areas Commun.*, vol. 32, no. 9, pp. 1637–1652, 2014.
- [2] S. Li and R. D. Murch, “An Investigation into Baseband Techniques for Single-Channel Full-Duplex Wireless Communication Systems,” *IEEE Trans. Wirel. Commun.*, vol. 13, no. 9, pp. 4794–4806, 2014.
- [3] A. Goldsmith, *Wireless Communications*. New York, NY, USA: Cambridge University Press, 2005.
- [4] B. van Liempd *et al.*, “RF Self-Interference Cancellation for Full-Duplex,” *Proc. 9th Int. Conf. Cogn. Radio Oriented Wirel. Networks*, 2014.
- [5] J. Il Choi, M. Jain, K. Srinivasan, P. Levis, and S. Katti, “Achieving Single Channel, Full Duplex Wireless Communication,” in *Proceedings of the Sixteenth Annual International Conference on Mobile Computing and Networking*, 2010, pp. 1–12.
- [6] A. Masmoudi and T. Le-Ngoc, *Full-Duplex Wireless Communications Systems: Self-Interference Cancellation*, 1st ed. Cham: Springer, 2017.
- [7] Y. S. Choi and H. Shirani-Mehr, “Simultaneous Transmission and Reception: Algorithm, Design and System Level Performance,” *IEEE Trans. Wirel. Commun.*, vol. 12, no. 12, pp. 5992–6010, 2013.
- [8] M. Amjad, F. Akhtar, M. H. Rehmani, M. Reisslein, and T. Umer, “Full-Duplex Communication in Cognitive Radio Networks: A Survey,” *IEEE Commun. Surv. Tutorials*, vol. 19, no. 4, pp. 2158–2191, 2017.
- [9] D. Korpi, T. Riihonen, V. Syrjälä, L. Anttila, M. Valkama, and R. Wichman, “Full-duplex transceiver system calculations: Analysis of ADC and linearity challenges,” *IEEE Trans. Wirel. Commun.*, vol. 13, no. 7, pp. 3821–3836, 2014.
- [10] H. Yang, H. Zhang, J. Zhang, and L. Yang, “Digital Self-Interference Cancellation Based on Blind Source Separation and Spectral Efficiency Analysis for the Full-Duplex Communication Systems,” *IEEE Access*, vol. 6, pp. 43946–43955, 2018.
- [11] G. Liu, F. R. Yu, H. Ji, V. C. M. Leung, and X. Li, “In-Band Full-Duplex Relaying: A Survey, Research Issues and Challenges,” *IEEE Commun. Surv. Tutorials*, vol. 17, no. 2, pp. 500–524, 2015.
- [12] D. Kim, H. Lee, and D. Hong, “A Survey of In-Band Full-Duplex Transmission: From the Perspective of PHY and MAC Layers,” *IEEE Commun. Surv. Tutorials*, vol. 17, no. 4, pp. 2017–2046, 2015.
- [13] H. Alves, R. D. Souza, and M. E. Pellenz, “Brief Survey on Full-Duplex Relaying and its Applications on 5G,” *2015 IEEE 20th Int. Work. Comput.*

- Aided Model. Des. Commun. Links Networks, CAMAD 2015*, pp. 17–21, 2016.
- [14] Z. Zhang, K. Long, A. V. Vasilakos, and L. Hanzo, “Full-Duplex Wireless Communications: Challenges, Solutions, and Future Research Directions,” *Proc. IEEE*, vol. 104, no. 7, pp. 1369–1409, 2016.
- [15] C. D. Nwankwo, L. Zhang, A. Quddus, M. A. Imran, and R. Tafazolli, “A Survey of Self-Interference Management Techniques for Single Frequency Full-Duplex Systems,” *IEEE Access*, vol. 6, no. c, pp. 30242–30268, 2018.
- [16] M. Jain *et al.*, “Practical, Real-time, Full-Duplex Wireless,” in *Proceedings of the 17th Annual International Conference on Mobile Computing and Networking*, 2011, pp. 301–312.
- [17] R. Askar, T. Kaiser, B. Schubert, T. Haustein, and W. Keusgen, “Active Self-Interference Cancellation Mechanism for Full-Duplex Wireless Transceivers,” in *2014 9th International Conference on Cognitive Radio Oriented Wireless Networks and Communications (CROWNCOM)*, 2014, pp. 539–544.
- [18] D. Bharadia, E. McMilin, and S. Katti, “Full-Duplex Radios,” *Proc. ACM SIGCOMM 2013 Conf. SIGCOMM - SIGCOMM '13*, p. 375, 2013.
- [19] M. Emara, P. Rosson, K. Roth, and D. Dassonville, “A Full-Duplex Transceiver with Reduced Hardware Complexity,” *2017 IEEE Glob. Commun. Conf. GLOBECOM 2017 - Proc.*, vol. 2018-Janua, pp. 1–6, 2018.
- [20] J. Li, H. Zhang, and M. Fan, “Digital Self-Interference Cancellation Based on Independent Component Analysis for Co-Time Co-frequency Full-Duplex Communication Systems,” *IEEE Access*, vol. 5, pp. 10222–10231, 2017.
- [21] M. S. Amjad, H. Nawaz, K. Ozsoy, O. Gurbuz, and I. Tekin, “A Low-Complexity Full-Duplex Radio Implementation with a Single Antenna,” *IEEE Trans. Veh. Technol.*, vol. 67, no. 3, pp. 2206–2218, 2018.
- [22] X. Wu, Y. Shen, and Y. Tang, “The Power Delay Profile of the Single-Antenna Full-Duplex Self-Interference Channel in Indoor Environments at 2.6 GHz,” *IEEE Antennas Wirel. Propag. Lett.*, vol. 13, pp. 1561–1564, 2014.
- [23] A. Balatsoukas-Stimming, P. Belanovic, K. Alexandris, and A. Burg, “On self-interference suppression methods for low-complexity full-duplex MIMO,” in *Conference Record - Asilomar Conference on Signals, Systems and Computers*, 2013, no. 1, pp. 992–997.
- [24] T. Huusari, Y. Choi, P. Liikkanen, D. Korpi, S. Talwar, and M. Valkama, “Wideband Self-Adaptive RF Cancellation Circuit for Full-Duplex Radio: Operating Principle and Measurements,” in *2015 IEEE 81st Vehicular Technology Conference (VTC Spring)*, 2015, pp. 1–7.
- [25] S. Khaledian, F. Farzami, B. Smida, and D. Erricolo, “Inherent Self-Interference Cancellation for In-Band Full-Duplex Single-Antenna Systems,” *IEEE Trans. Microw. Theory Tech.*, vol. 66, no. 6, pp. 2842–2850, 2018.

- [26] S. Hong, J. Mehlman, and S. Katti, “Picasso: Flexible RF and Spectrum Virtualization,” *Proc. ACM SIGCOMM*, 2012.
- [27] V. Tapio and M. Sonkki, “Analog and Digital Self-Interference Cancellation for Full-Duplex Transceivers,” in *European Wireless 2016; 22nd European Wireless Conference*, 2016, pp. 1–5.
- [28] M. E. Knox, “Single Antenna Full-Duplex Communications Using a Common Carrier,” *2012 IEEE 13th Annu. Wirel. Microw. Technol. Conf. WAMICON 2012*, 2012.
- [29] P. Semiconductors, “Circulators and Isolators, Unique Passive Devices,” Eindhoven, AN98035, 1998.
- [30] D. Korpi *et al.*, “Full-Duplex Mobile Device: Pushing the Limits,” *IEEE Commun. Mag.*, vol. 54, no. 9, pp. 80–87, 2016.
- [31] J. Zhang, O. T. Motlagh, J. Luo, and M. Haardt, “Full-Duplex Wireless Communications with Partial Interference Cancellation,” *Conf. Rec. - Asilomar Conf. Signals, Syst. Comput.*, pp. 1295–1299, 2012.
- [32] D. Korpi, T. Huusari, Y. S. Choi, L. Anttila, S. Talwar, and M. Valkama, “Digital Self-Interference Cancellation Under Nonideal RF Components: Advanced Algorithms and Measured Performance,” *IEEE Work. Signal Process. Adv. Wirel. Commun. SPAWC*, vol. 2015-August, pp. 286–290, 2015.
- [33] E. Ahmed and A. M. Eltawil, “All-Digital Self-Interference Cancellation Technique for Full-Duplex Systems,” *IEEE Trans. Wirel. Commun.*, vol. 14, no. 7, pp. 3519–3532, 2015.
- [34] K. B. King, “Digitally-Assisted RF-Analog Self Interference Cancellation for Wideband Full-Duplex Radios,” 2016.
- [35] M. Duarte and A. Sabharwal, “Full-Duplex Wireless Communications Using Off-the-Shelf Radios: Feasibility and First Results,” in *Conference Record - Asilomar Conference on Signals, Systems and Computers*, 2010, pp. 1558–1562.
- [36] K. Haneda, E. Kahra, S. Wyne, C. Icheln, and P. Vainikainen, “Measurement of Loop-Back Interference Channels for Outdoor-to-Indoor Full-Duplex Radio Relays,” *Antennas Propag. (EuCAP), 2010 Proc. Fourth Eur. Conf.*, pp. 1–5, 2010.
- [37] F. Luo and C. (Jianzhong) Zhang, *Signal Processing for 5G: Algorithms and Implementations*, 1st ed. Chichester: Wiley-IEEE Press, 2016.
- [38] E. Everett, M. Duarte, C. Dick, and A. Sabharwal, “Empowering Full-Duplex Wireless Communication by Exploiting Directional Diversity,” in *Conference Record - Asilomar Conference on Signals, Systems and Computers*, 2011, pp. 2002–2006.
- [39] E. Everett, A. Sahai, and A. Sabharwal, “Passive Self-Interference Suppression

- for Full-Duplex Infrastructure Nodes,” *IEEE Trans. Wirel. Commun.*, vol. 13, no. 2, pp. 680–694, 2014.
- [40] C. Goodbody, T. Karacolak, and N. Tran, “Dual-Polarised Patch Antenna for In-Band Full-Duplex Applications,” *Electron. Lett.*, vol. 54, no. 22, pp. 1255–1256(1), Nov. 2018.
- [41] T. Huusari, “Analog RF Cancellation of Self Interference in Full-Duplex Transceivers,” 2014.
- [42] E. Manuzzato, J. Tamminen, M. Turunen, D. Korpi, F. Granelli, and M. Valkama, “Digitally-Controlled Electrical Balance Duplexer for Transmitter-Receiver Isolation in Full-Duplex Radio,” *Eur. Wirel. Conf.*, pp. 210–217, 2016.
- [43] B. Van Liempd, B. Hershberg, B. Debaillie, P. Wambacq, and J. Craninckx, “An Electrical-Balance Duplexer for In-Band Full-Duplex with  $<-85$ dBm In-Band Distortion at +10dBm TX-Power,” *Eur. Solid-State Circuits Conf.*, vol. 2015-Octob, pp. 176–179, 2015.
- [44] L. Laughlin, C. Zhang, M. A. Beach, K. A. Morris, and J. Haine, “A Widely Tunable Full duplex Transceiver Combining Electrical Balance Isolation and Active Analog Cancellation,” *IEEE Veh. Technol. Conf.*, vol. 2015, 2015.
- [45] J. R. Krier and I. F. Akyildiz, “Active Self-Interference Cancellation of Passband Signals Using Gradient Descent,” *IEEE Int. Symp. Pers. Indoor Mob. Radio Commun. PIMRC*, pp. 1212–1216, 2013.
- [46] A. Sahai, G. Patel, and A. Sabharwal, “Pushing the Limits of Full-duplex: Design and Real-time Implementation,” *CoRR*, vol. abs/1107.0, 2011.
- [47] D. Korpi, *Full-Duplex Wireless: Self-interference Modeling, Digital Cancellation, and System Studies*. Tampere University of Technology, 2017.
- [48] J. Tamminen *et al.*, “Digitally-Controlled RF Self-Interference Canceller for Full-Duplex Radios,” *Eur. Signal Process. Conf.*, vol. 2016-Novem, pp. 783–787, 2016.
- [49] D. Korpi, Y. S. Choi, T. Huusari, L. Anttila, S. Talwar, and M. Valkama, “Adaptive Nonlinear Digital Self-Interference Cancellation for Mobile Inband Full-Duplex Radio: Algorithms and RF Measurements,” *2015 IEEE Glob. Commun. Conf. GLOBECOM 2015*, 2015.
- [50] M. Emara, K. Roth, L. G. Baltar, M. Faerber, and J. Nossek, “Nonlinear Digital Self-Interference Cancellation with Reduced Complexity for Full Duplex Systems,” in *WSA 2017; 21th International ITG Workshop on Smart Antennas*, 2017, pp. 1–6.
- [51] M. S. Amjad and O. Gurbuz, “Linear Digital Cancellation with Reduced Computational Complexity for Full-Duplex Radios,” *IEEE Wirel. Commun. Netw. Conf. WCNC*, no. 215, 2017.

- [52] C. Li, H. Zhao, F. Wu, and Y. Tang, “Digital Self-Interference Cancellation with Variable Fractional Delay FIR Filter For Full-Duplex Radios,” *IEEE Commun. Lett.*, vol. 22, no. 5, pp. 1082–1085, 2018.
- [53] S. Li and R. D. Murch, “Full-Duplex Wireless Communication Using Transmitter Output Based Echo Cancellation,” *GLOBECOM - IEEE Glob. Telecommun. Conf.*, 2011.
- [54] D. Korpi, L. Anttila, and M. Valkama, “Reference Receiver Based Digital Self-Interference Cancellation in MIMO Full-Duplex Transceivers,” in *2014 IEEE Globecom Workshops, GC Wkshps 2014*, 2014, pp. 1001–1007.
- [55] T. J. Roupael, *Wireless Receiver Architectures and Design: Antennas, RF, Synthesizers, Mixed Signal, and Digital Signal Processing*. Boston: Academic Press, 2014.
- [56] P. Baudin, *Wireless Transceiver Architecture: Bridging RF and Digital Communications*. Chichester, UK: John Wiley & Sons, Ltd, 2014.
- [57] S. Mirabbasi and K. Martin, “Classical and Modern Receiver Architectures,” *IEEE Commun. Mag.*, vol. 38, no. 11, pp. 132–139, 2000.
- [58] B. Razavi, “Architectures and Circuits for RF CMOS Receivers,” *Proc. Cust. Integr. Circuits Conf.*, pp. 393–400, 1998.
- [59] B. Razavi, “Design Considerations for Direct-Conversion Receivers,” *IEEE Trans. Circuits Syst. II Analog Digit. Signal Process.*, vol. 44, no. 6, pp. 428–435, 1997.
- [60] A. A. Abidi, “Direct-Conversion Radio Transceivers for Digital Communications,” *Integr. Circuits Wirel. Commun.*, vol. 30, no. 12, pp. 135–146, 1998.

## APPENDIX: SYSTEM SIMULATION CONFIGURATIONS

### SI Source Model Configurations

Block	Parameter		Value
Bernoulli Binary	Probability of a zero		0.5
	Initial seed		61
	Sample time (s)		1/(5e6)
	Output data type		Double
BPSK	Phase offset (rad)		0
	Output data type		Double
Raised Cosine Transmit Filter	Filter shape		Square root
	Rolloff factor		0.2
	Filter span in symbols		10
	Output samples/symbol		10
	Linear amplitude filter gain		1
	Input processing		Elements as channels
Complex to Real- Imag	Output		Real and imag
Reconstruction Filter (Analog Filter Design)	Design method		Elliptic
	Filter type		Lowpass
	Passband edge frequency (rad/s)		$20*\pi*e6$
	Passband ripple (dB)		0.5

	Stopband attenuation		60
Real-Imag to Complex	Input		Real and imag
Resample (Zero-Order Hold)	Sample time (s)		1/(32e6)
Power Calibration (dB gain)	Gain (dB)		User-adjustable

### SOI Source Model Configurations

Block	Parameter	Value
Bipolar Bit Generator (Bernoulli Binary Generator)	Probability of a zero	0.5
	Initial seed	61
	Sample time (s)	1/(2.5e5)
	Output data type	Double
PN Generator (PN Sequence Generator)	Generator Polynomial	[0 -7 -10]
	Initial States	[1 0 0 0 0 0 0 0 0]
	Sample Time (s)	1/(2e6)
QPSK	Input Type	Bit
	Constellation Ordering	Gray
	Phase offset (rad)	Pi/4
	Output data type	Double
Half Sin Filter	Coefficient Source	Dialogue parameters
	FIR filter coefficients	1x32 matrix

	Interpolation Factor	32
	Input processing	Elements as channels
	Output Buffer Initial Conditions	0
	Input processing	Elements as channels
Q Branch Timing Offset to O-QPSK		
Complex to Real-Imag	Output	Real and imag
Inter Delay	Delay Length	16
	Initial Condition	0.0
	Input Processing	Elements as Channels
	External Reset	None
	Sample time	Inherited
Real-Imag to Complex	Input	Real and imag
Power Calibration (dB gain)	Gain (dB)	User adjustable

### PSIC Model Configurations

<b>Circulator</b>		
<b>Block</b>	<b>Parameter</b>	<b>Value</b>
Attenuator	Attenuation (dB)	20
	Input impedance (Ohm)	50
	Output impedance (Ohm)	50

Transmission Line	Model type	Delay based and lossless
	Transmission Delay (s)	400e-12
	Characteristic impedance (Ohm)	50
<b>Antenna Reflection</b>		
<b>Block</b>	<b>Parameter</b>	<b>Value</b>
Attenuator	Attenuation (dB)	20
	Input impedance (Ohm)	50
	Output impedance (Ohm)	50
Transmission Line	Model type	Delay based and lossless
	Transmission Delay (s)	1.4e-9
	Characteristic impedance (Ohm)	50
<b>Environmental Reflections</b>		
<b>Block</b>	<b>Parameter</b>	<b>Value</b>
Outport	Sensor type	Power
	Load impedance (Ohm)	50
	Output	Complex Baseband
Outport	Carrier Frequencies (GHz)	2.45
SISO Fading Channel (Main)	Discrete path delays (s)	[7e-7, 8e-7, 9e-7, 10e-7]
	Average path gains (dB)	[-86,-89,-92,-95]
	Fading distribution	Rayleigh
	Maximum Doppler shift (Hz)	245

	Doppler spectrum	doppler('Jakes')
	Initial seed	73
	Simulate using	Interpreted execution
SISO Fading Channel (Visualisation)	Channel visualisation	Off
Loop break (Delay)	Delay length(Source: Dialog)	1
	Initial condition (Source: Dialog)	1
	Input processing	Elements as channels (sample-based)
	External reset	none
	Sample time	-1
	Initial seed	73
Inport	Source type	Power
	Source impedance (Ohm)	50
	Carrier frequencies (GHz)	2.45

### AASIC Model Configurations

<b>Circulator Leakage Cancellation Path</b>		
<b>Block</b>	<b>Parameter</b>	<b>Value</b>
Attenuator	Attenuation (dB)	20
	Input impedance (Ohm)	50
	Output impedance (Ohm)	50

Transmission Line	Model type	Delay based and lossless
	Transmission Delay (s)	400e-12
	Characteristic impedance (Ohm)	50
Phase shift	Phase shift (degree)	180
<b>Antenna Reflection Cancellation Path</b>		
<b>Block</b>	<b>Parameter</b>	<b>Value</b>
Attenuator	Attenuation (dB)	20
	Input impedance (Ohm)	50
	Output impedance (Ohm)	50
Transmission Line	Model type	Delay based and lossless
	Transmission Delay (s)	1.4e-9
	Characteristic impedance (Ohm)	50
Phase shift	Phase shift (degree)	180